ABSTRACT

Title of Thesis: THE *MEIOTIC PROPHASE AMINOPEPTIDASE 1* REGULATES POLYPLOIDY IN *ARABIDOPSIS THALIANA*

Kasuni Vishwaprabha Wattarantenne, Master of Science, 2017

Thesis Directed By: Dr. Wendy Ann Peer, Assistant Professor, Department of Environmental Science and Technology

Growth and development in plants is dependent on cellular functions such as cell cycle progression. M1 aminopeptidases have been shown to regulate mitosis and meiosis in animals. *MEIOTIC PROPHASE AMINOPEPTIDASE 1* (*MPA1*) in *Arabidopsis thaliana* was previously shown to regulate cell cycle progression during prophase I in meiosis I in both female and male gametophytes and be essential for homologous recombination. *mpa1* homozygous embryos are lethal due to chromosome de-synapsis resulting in uneven distribution of chromosomes in daughter cells and massive decrease in homologous crossovers reduces independent assortment. Here, I show that MPA1 is a soluble protein and is expressed throughout the seedling: in the primary root, hypocotyl, cotyledons, petioles and root and shoot apical meristem. I isolated and characterized four *mpa1* alleles, and I showed that *MPA1* loss-of-function mutants exhibited three significant phenotypes corresponding

to development in seedlings and adult plants in Arabidopsis: non-disjunction in mitotic cells, altered polyploidy, and temporary arrest of primary root growth during seedling establishment.

The *MEIOTIC PROPHASE AMINOPEPTIDASE 1* regulates polyploidy in *Arabidopsis thaliana*

by

Kasuni Vishwaprabha Wattarantenne

Thesis submitted to the Faculty of the Graduate School of the
University of Maryland, College Park, in partial fulfillment
of the requirements for the degree of
Master of Science
2017

Advisory Committee:
Dr. Wendy Ann Peer, Chair
Dr. Angus Murphy
Dr. Gary Coleman

Preface

This thesis contains my research work in pursuance of a Master's of Science degree. Here, I focused on elucidating the role of *MPA1* in seed and seedling establishment via mitosis cell cycle regulation. MPA1 is a cytosolic protein and it was previously identified as a regulator of the meiotic cell cycle. *MPA1* encodes a protein that is essential for homologous recombination, synapsis, and further, it was recognized as facilitating chromosome disjunction of homologous univalents in anaphase I. *MPA1* expression in 5-day old seedlings was examined using a native promoter driving expression of a functional fluorescent protein fusion (Pro*MPA1*: MPA1- YFP) via confocal laser scanning microscopy. Pro*MPA1*: MPA1- YFP signals indicated moderate expression in root apical meristem including root cap, lateral root cap, epidermis, and quiescent center. In cotyledons, moderate expression was observed in guard cells and epidermal cells. Further, I analyzed *MPA1* loss-of-function mutants for polyploidy and developmental phenotypes. Four *mpa1* alleles were isolated and characterized. Three significant phenotypes corresponding to development in young seedlings and seeds in *Arabidopsis thaliana* were observed:1) MPA1 regulate chromosome disjunction in mitotic cells, 2) As a result chromosome non disjunction, *mpa1* exhibited altered ploidy,3) Temporary arrest of primary root growth during seedling establishment is due to post transcriptional/post translational regulation of *MPA1* gene expression. These results indicated that MPA1 participates in mitosis regulatory mechanism in a similar way to meiosis. In my first chapter, I present a review of cell cycle regulatory genes, the relatedness of cell cycle to polyploidy, and the M1 peptidases in animal and plant kingdoms that are known to regulate cell cycle

progression. In my second chapter I investigated whether MPA1 regulates mitosis cell cycle by controlling chromosome disjunction. Therefore, I analyzed *mpa1* mutant seedling and they exhibited temporary primary root growth arrest at 5 days. However, the root grew continuously after 5 days and eventually reached the root length of Col-0 at 7 days. I hypothesized that this might be due post-transcriptional or post-translational regulation of *MPA1* expression. In addition to that, 35S:CEHN3-GFP localization in dividing root cells of *mpa1* indicated chromosome non–disjunction. Further, flow cytometry of *mpa1* cotyledons showed a decrease in 4C values supporting the hypothesis MPA1 regulates chromosome disjunction and acts as a negative regulator of ploidy.

Dedication

This dissertation is dedicated to my husband, Shavindra Premaratne. I give my deepest expression of love and appreciation for the encouragement that you gave and the sacrifices you made during this graduate program.

Acknowledgements

Foremost, I would like to express my sincere gratitude to my advisor Dr. Wendy Ann Peer for the continuous support of my Master of Science research, for her patience, motivation, enthusiasm, and immense knowledge. Her guidance helped me in all the time of research and writing of this thesis.

Besides my advisor, I would like to thank the rest of my thesis committee: Dr. Angus Murphy and Dr. Gary Coleman for their encouragement and insightful comments.

My sincere thanks also goes to Omair Khan for helping me with genotyping and Rama Al-Shalabi for taking care of my transgenic plants.

I thank my fellow lab mates Reuben Tayengwa, Changxu Pang, Jun Zhang, Mark Jenness, Candace Prichard, Chinchu Harris, and my best friend in the lab Sarah Turner.

I would also like to thank our lab interns Gabrielle Bate, Michael Laskowski, Uma Krishnan, Sarah Miller, Jongmi Park, Ryan Parker and Denise Alving.

I would like to express my special gratitude for Julie Caruana for helping me with cloning and construction of transgenic lines.

I would like to thank Xiping Liu for developing *MPA1* overexpression construct (35S-*MPA1*-CFP).

Last but not least, I would like to thank my parents and my brother for providing me with unfailing support and continuous encouragement throughout my years of study. This accomplishment would not have been possible without them.

Table of Contents

List of Tables

List of Figures

Chapter 1: Literature Review: M1 metallopeptidases and their function in cell cycle regulation.

The M1 metalloprotease family selectively remove amino acids from the N-terminus of peptide chains. M1 metalloproteases are encoded by multigene families and are found across almost all kingdoms including animalia, plantae, fungi, protozoa and kingdom apicomplexan. M1 protease activity requires zinc, and therefore, M1 proteases are also known as gluzicins. M1 proteases have two highly conserved signature motifs located in the catalytic domain: the zinc-binding motif HEXXH and the exopeptidase motif GXMEN are known to be essential for their catalytic activity. M1 peptidases play a variety of roles in multiple physiological processes including protein maturation, protein turnover and regulation of peptide hormone levels. M1 peptidases are also found in multiple subcellular compartments and in extracellular spaces. Further, M1 proteases exhibit tissue-specific functionality. M1 proteases have been shown to have roles in meiosis and mitosis in plants and animals which is the subject of this review.

Genes in cell cycle regulation

The cell cycle is a complex process that comprises of series of cytoplasmic and nuclear events which are well coordinated. Mitosis is the process whereby the replicated chromosomes migrate to two nuclei and the cytoplasm divides to produce two identical daughter cells. Meiosis is the combination of two cell division events in which the

chromosome number reduces to half to produce gametes. The ultimate result is four daughter cells which are genetically unique and non-identical to the mother cell. Both meiotic and mitotic cell cycles are comprised of series of stages starting from Gap 0 (G0), Gap 1 (G1), synthesis (S), Gap two (G2) and mitosis (M) [1]. In G0 the cell cycle is halted, and here healthy cells rest with no further cell division and unhealthy cells undergo apoptosis. Diving cells have three unique cell cycle checkpoint correction mechanisms to detect if any errors occurred during DNA replication to prevent the cells from entering the next stage of the cell cycle. The checkpoints occur during G1, G2 and spindle assembly [2]. In G1, the cells grow larger and organelles duplication occurs, and in S phase, the cells synthesize complete copies of genomic DNA. In G2, protein synthesis take places and the cells become even larger and prepare for M phase [3].

The M phase is the final stage of the cell cycle that further divided into four stages followed by cytokinesis. The mitotic spindle forms in prophase. In metaphase, microtubules bind to centrosomes at the equator of the cell, and in anaphase, microtubules pull chromosomes towards the opposite ends of the cell. Later in anaphase, the sister chromatids migrate to opposite ends of the cell followed by telophase. In telophase, the nuclear envelope re-forms, and the nucleolus reappears. As the last step of the cell cycle, cells reach cytokinesis in which cytoplasm division takes place [4]. Cytokinesis ensures that nuclei and organelles move to each daughter cell except in a scenario like endoreduplication [5].

The regulation of cell proliferation is important for growth, development and reproduction in higher plants. Progression thorough the cell cycle phases is facilitated by heterodimeric serine or threonine protein kinases. These kinases are comprised of two

subunits, a catalytic subunit, termed cyclin-dependent kinase (CDK), and an activating subunit, called cyclin [6]. The *Arabidopsis thaliana* genome contains 38 cyclin related genes and many of them function in cell cycle regulation [7]. They are crucial for spindle assembly and function, chromosome segregation, mitotic checkpoint control, and cytokinesis [8]. CDKs are categorized into seven groups, CDKA to CDKG [6], and are key cell cycle regulators that have been widely used as mitotic markers [9]. CDKAs and CDKBs are critical for cell cycle progression. CDKAs are required for S phase entry and quiescent center maintenance. CDKBs are only found in plants, and they belong to two subfamilies named B1 and B2. B1s are expressed from S phase to M phase. *CDKB1* transcription occurs during S, G2, and M phases, but *CDKB2* expression is restricted to G2 and M phases [7], and is specifically expressed in the sub-phase between G2 to M and function in the meristem organization [6],[9]. CDKB2s function in leaf and guard cell development, thus reduced CDKB2 activity causes decreased stomatal index, and a blocked G2 phase gives rise to abnormally shaped guard cells [7]. *CDKB*s are highly expressed in meristematic regions and loss of function *cdkb2;*1 and *cdkb2;2* exhibit severe defects in meristematic region together with alterations in hormone signaling pathways[10].

Cyclins bind to CDKs and control the timing of CDK activation [11]. Cyclins are categorized into two major groups: gap 1 (G1) and mitotic (M) specific cyclins. Doerner and colleagues work on the Arabidopsis mitotic cyclin CYCB1;1 demonstrated that it is an important regulator for cell division in Arabidopsis [9]. G1 and M phases can be delayed by *CYCB1;1* transcriptional and post-translational regulation. Thus, it is extensively used as a cell cycle marker to study mitosis [9]. D-type cyclins (CycD)

promote cell proliferation in response to external cues [12]. CYCD2 and CYCD3 regulate the cell cycle in presence of sugar as the carbon source [13]; sucrose is the major carbon source produced and transported in plants and that acts as one of the key determinant factors influences cell division [12].

Transcription factors also regulate the cell cycle, such as Retinoblastoma (Rb) and E2 Factor (E2F). Rb, the first tumor suppressor identified, and E2F interact to play a crucial role in regulating cell cycle during the G1 to S transition [13]. The transcriptional activation of *E2F* is required for cell cycle progression, and Rb arrests cells in G1 by inhibiting *E2F* transcriptional activity [14] [15]. E2F binds to genes encoding proteins involved in chromatin assembly, chromosome condensation and regulate transcription and cell-cycle progression [16]. Further, direct target genes of E2Fa and E2Fb are required for DNA replication and DNA repair [17] that take place during interphase. pRB binds to E2F and converts E2Ffrom a transcriptional activator to a transcriptional repressor. The E2F–Rb signaling pathway governs the G1/S-phase transition by activation of genes required in DNA synthesis and cell-cycle regulation, such as *F-BOX-LIKE 17 (FBL17)* and *CELL DIVISION CONTROL 6 (CDC6)*[18] RB is a target of CDK, and CDKs inactivate RB which then interferes with the cell entry into S phase in mammals [19].

The retinoblastoma (Rb) homolog of Arabidopsis RB-RELATED1 (RBR1) appears to control cell proliferation, differentiation, stem cell niche maintenance, endoreduplication, and cell size in the endosperm of maize [5] [20]. RBR1 and the transcription factor SCARECROW regulate specific stem cell divisions that helps to protect cells against stress-induced cell death [20]. RBR1 is also essential for chromosome condensation and

synapsis of homologous chromosomes in meiosis [20]. In Arabidopsis, RBR1 function depends on CDKB1 activity, and RBR1 is also required for DNA repair, and its. In addition , RBR1 has a cell cycle-independent function in DNA repair as *rbr1* mutants treated with roscovitine which specifically inhibits Cdk1/2-type kinases and leads to cell death [21]. DNA damage in multicellular organisms often leads to one of these three major responses: arrest of cell division followed by repair of the damage terminal differentiation and exit from the cell cycle, or apoptosis [21].

Asymmetric cell division is critical for establishment of the cellular patterns in plants, such as the cortex and endodermis. Two transcription factors SHORT-ROOT (SHR) and SCARECROW (SCR) are essential for tissue patterning during root development [22]. These proteins play a role in periclinal asymmetric cell division which produces distinct cell files [22].

Members from M1 metalloprotease family have also been identified as key factors in cell cycle progression in mitosis and meiosis. They will be discussed below.

Arrested cell cycle and cytokinesis result in polyploidy

Failures in mitosis or meiosis, more particularly, mis-segregation of chromosomes in anaphase, give rise to polyploidy or aneuploidy conditions in both plants and animals [23]. Aneuploidy is a loss or gain of chromosomes compared to the normal chromosome set, and duplication of the whole genome is known as polyploidy. Both these events can eventually lead to visible phenotypes in organisms [24]. Aneuploidy and polyploidy can be directly related to interphase and anaphase, chromosome arrangement, and dynamics [25]. Chromosomal imbalance describes the phenomenon of addition or subtraction of

chromosome(s) or sections of chromosomes in the nucleus. In addition to aneuploidy, whole genome duplication, chromosome segmental duplications [26], tandem duplications, and gene copy number variation can contribute to chromosome imbalance [27]. However, the natural mechanisms of polyploidy and aneuploidy remain unclear. In plants, it is hypothesized that the most common mechanism for polyploidy is mis-segregated chromosomes following gamete fusion and fertilization [27]. The fusion of an unreduced gamete with a haploid gamete forms a triploid bridge (triploid intermediate) followed by the union of the triploid gamete with a haploid gamete that produces a tetraploid [28], [29]. In contrast, endoreduplication can be achieved by an alteration in the mitotic cell cycle. One of the many circumstances is that the mitotic cell cycle is skipped due to mis-communication between regulatory mechanisms and cell cycle checkpoints, which permits cells to replicate DNA excessively. This transpires when CDK activity is maintained below the threshold required for mitosis [7].

The mitotic cell cycle can be arrested at different sub-stages of the cycle. Fungicides, organic solvents, anesthetics and anticancer drugs are used to arrest cells in metaphase [23]. This cessation can take place due to polymerization of tubulin and inhibition of centriole separation [23]. The effects of some of these arrestants, such as colcemid, can be reversed when the reagent is removed [23]. Further, immunohistochemical studies of mouse cells indicated that in megakaryocytes, mitosis progresses through prophase, prometaphase, and metaphase until it reaches anaphase A, but the treated cells do not reach anaphase B, telophase, or cytokinesis [30]. In anaphase A, the chromosomes move to the opposite spindle poles, and kinetochores microtubules become shortened. In anaphase B, the spindle poles separate from each other and move to opposite ends of the

cell [31]. During thrombopoietin-induced polyploidization, spindle pole pairs in anaphase remained close to each other [30], and Nagata et al. assumed that it was due to lack of outward movement of spindle poles in anaphase B [30]. Based on these data, they concluded that polyploidization in megakaryocytes occurs not only by skipping mitosis, but also due to a unique regulatory mechanism in anaphase [30].

Chromosome non-disjunction is when homologous chromosomes or sister chromatids fail to separate during cell division. Cohesin is a chromosome binding protein complex which mediates cohesion between sister chromatids in mitosis [32]. Thus, hydrolysis of cohesin is mediated by the cysteine protease called separase [32] [33]. Separase is activated by the anaphase-promoting complex (APC) in metaphase. Loss of separase function at certain temperatures results in chromosomes replication defects and chromosome non-disjunction [33].

However, genome doubling or gain- or loss-of-chromosomes does not always result in an increase in cell size. Experimental data showed that was no difference in the biomass of a tetraploid and a triploid produced from a diploid mother plant *Dactylis glomerata* [34], but subtle morphological variations such as larger or smaller fruit size were observed occasionally in plants [35]. Polyploids are often successful in new and disturbed ecosystems[36]. Most of them show better fitness than their diploid progenitor in such habitats [36]. For example, tetraploid *Gossypium hirsutum* (cotton) is a well-established plant in warmer, semi-arid environments in the world, but the diploid progenitor show less vigor in stressful environments [37]. Polyploidy often results in heterosis, also called hybrid vigor, in which hybrids show better fitness and vigor than their parents which contributes to the success of the hybrids. For example, many genes are expressed

differently in the parent and hybrids in maize which leads to increased vigor compared to the parental plants [38] Further, gene redundancy can protect polyploids from the deleterious effect of mutations [39]. However, there are certain disadvantages that account for polyploidization. In some instances, the increased genetic material causes the cell volume to increase. In such situations, the cellular architecture changes, and that can cause cellular homeostatic and regulatory problems such as higher cellular metabolic rates [40]. Further, difficulties in meiosis can also occur. For example, resolution of multivalents or tetravalents in anaphase I is very difficult compared to bivalents, and can result in abnormal chromosome segregation ratios like ‘3:1’ or ‘2:1’ plus one laggard [41].

M1 aminopeptidases

M1 proteases are zinc-dependent peptidases, also known as gluzincins. M1 protease encoding genes are divided into groups based on the mode of action, such as the pH optimum for catalytically activity and the amino acid preference at the cleavage site. Peptidases that cleave internal peptide bonds are called endopeptidases, and exopeptidases hydrolyze the peptide chain at the N-terminus and carboxypeptidases cleaves the peptide chain at the C-terminus, and they are categorized as aminopeptidases and carboxypeptidases, respectively. . The zinc ligand is bound by the histidines in the highly conserved motif, HEXXH, and a glutamate which is a catalytic residue [42]. M1 aminopeptidases show N-terminal processing that cleaves single amino acid or a series of amino acids. The highly conserved GXMEN motif is essential for catalytic activity and substrate recognition of M1 metallopeptidases [43].

M1 peptidases are commonly found in plant, animal, fungi [44] protozoa [45] and apicomplexa [46] kingdoms to date. Fifty-five different M1 proteases are predicted in Archaea, Bacteria and Eukaryotes and 12 different enzymes are well-characterized [47]. M1 aminopeptidases are also known to regulate cellular processes such as the cell cycle, and cellular maintenance, growth, defense and apoptosis [42]. For example MEIOTIC PROPHASE AMINOPEPTIDASE I (MPA1) regulates meiosis in Arabidopsis [48]. M1 peptidases are characterized by varying degrees of sensitivity to the inhibitor puromycin, which arrests eukaryotic cells in the G2/M phase [49]. PAQ-22/PIQ-22 and the auxin transport inhibitor 1-naphthylphthalamic acid (NPA) have pthalimide structure. These are puromycin-sensitive aminopeptidase inhibitors [50]. PAQ-22 indicates the PSA-specific noncompetitive inhibitory activity. These arrest mitosis cell cycle, thus they are used as anti-cancer drugs to treat mostly blood cancers/ leukemia suggesting that M1 peptidases have a function in cell cycle regulation.M1 members also participate in non-catalytic functions. For example AMINOPEPTIDASE M1 (APM1) regulates subcellular protein trafficking in Arabidopsis including the auxin export facilitator PIN2and the auxin transporter ABCB19[50] and cholesterol uptake is regulated by Aminopeptidase N (APN). When confluent $CaCO_2$ cells were treated with ezetimibe, a cholesterol uptake inhibitor, ezetimibe strongly bound APN, and APN signals decreased at the plasma membrane [51][52]. This indicated that ezetimibe blocked APN-mediated endocytosis of cholesterol- rich membrane micro-domains [51].

Loss of *MPA1* function in plants corresponds to reduced fertility and aneuploidy/ polyploidy as a result of chromosome mis-segregation in meiosis [48], [53], and mitosis (Chapter 2). Loss of *APM1* function results in mitotic cell cycle arrest and defects in

embryogenesis and seedling development. Correspondingly, loss-of-function *MPA1* homologous in animals correlates to decreased fertility via meiotic defects.

Figure 1. Graphical representation of common motifs in M1 metalloprotease protein structure. The signature enzymatic domains is colored in dark blue, hydrophobic domain in yellow and protein–protein interaction domains in red [49]. HEXXH(X18)E, the zinc binding domain, and GXMXN, exopeptidase domain are the consensus sequences found in the catalytic domain of M1 aminopeptidases. The protein-protein interaction and hydrophobic domains are not conserved throughout the family.

M1 metallopeptidases function in cell cycle regulation

Animal kingdom

Aminopeptidase N (APN, Alanyl aminopeptidase)

Aminopeptidase N, also known as CD13 is a type II integral membrane ectopeptidase that cleaves neutral and basic amino acids from the N-terminus of oligopeptides [54]. *APN/ CD13* expression is modulated during the cell cycle. *CD13* expression is decreased in cells that are entering S phase [55], and APN might have a function in human monocytoid cell proliferation by manipulating the rate of the cell cycle [55]. This suggests that *APN* may be a regulatory component of the cell cycle.CD13 is a cell surface

marker for malignant myeloid cells. APN is abundantly expressed in other tissues, such as intestinal epithelial, kidney, liver, blood monocytes, granulocytes and lung [56], and it is over-expressed in various mammalian tumor cells, melanoma, prostate, ovarian, colon, renal and pancreatic carcinomas which are results of excessive cell division [54]. Therefore, *APN* expression is high in tumor cells and tumor microenvironments where cell division is rapid and vigorous. APN is a therapeutic target in human liver cancer stem cells. Designer drugs bind to the APN active site and inhibit its enzymatic activity resulting in suppressed tumor growth [57].

In addition to tumor invasion and metastasis, APN also regulates angiogenesis via angiotensin III (Ang III) metabolism [54], [53]. APN converts Ang III to Ang IV [58]. Further, APN regulates inflammatory responses, which can be used as a marker to detect pathogenic diseases [56]. Orthologues of APN are also present in numerous apicomplexan parasites, including *Plasmodium*, *Toxoplasma*, *Cryptosporidium*, and *Eimeria* [46] and function in pathogenesis in humans.

Puromycin sensitive aminopeptidase (PSA)

The mammalian Puromycin Sensitive Aminopeptidase (PSA) was first M1 purified from brain tissues of rats [59]. Orthologs of PSA can be found in the genome of plants, mammals and multicellular organisms [59]. Mutations in PSA and PSA orthologues in the plant and animal kingdoms interfere with meiosis and gametogenesis, thereby negatively impacting reproductive success and fitness of organisms. Puromycin Sensitive Aminopeptidase M-1 (PAM-1) is the *Caenorhabditis elegans* orthologue of PSA. PAM-1 encodes a puromycin sensitive aminopeptidase that governs centrosome positioning in

early embryogenesis. PAM-1 promotes gametogenesis and fecundity in *C. elegans* and *pam-1* loss of function nematodes results in reduction in fertility [59]. In *pam-1* mutants, germ cell nuclei enter meiosis as soon as they complete mitosis, and remain in the pachytene stage in prophase I for an extended period of time. Further, the rate of oocyte nucleolus disassembly is decreased in *pam-1*. These two phenotypes negatively affect the embryonic viability and overall brood size in *C. elegans* [59].

PAM-1 is also cytosolic during early embryogenesis where it accumulates around mitotic centrosomes and chromosomes [60]. In *pam-1* null mutants, the centrosomes donated by sperm do not polarize the axis between anterior and the posterior of the oocyte because the centrosome does not remain at the posterior of the cell. [60]. These results indicate that *PAM-1* has a critical role in polarization of anterior-posterior axis by preventing the premature movement of the centrosome from the posterior cortex, which ensures the polarity in the *C. elegans* embryo [60]. The PSA orthologue from the planarian *Dugesia japonica, DjPsa,* is expressed in brain and ventral nerve cords of these animals. *DjPsa* exhibits tissue and developmental stage-specific expression patterns in developing embryos and larvae [61]. Additionally, *Drosophila melanogaster PSA* mutants display defects in spermatogenesis. These studies indicate the conservation of structure and function of PSA through evolution [62].

Cellular functions of M1 metallopeptidases in plant kingdom

Plant kingdom

Aminopeptidase M1 (APM1)

Arabidopsis Aminopeptidase M1 (APM1) is placed in the plant/animal/archaea clade of the family phylogenetic tree [49]. APM1 is a peripheral membrane protein first identified by its affinity for the auxin transport inhibitor 1-naphthylphthalamic acid (NPA) [63]. APM1 activity is sensitive to the G2/M phase inhibitor puromycin, and the anti-cancer drugs bestatin, apstatin and the phthalimides PAQ-22/PIQ-22 [49]. The experimental data indicate that both the catalytic and protein-protein interaction domains in APM1 are necessary for the APM1 dimer to function. However, the dimerization does not require these two domains to be present in the same linear molecule [49]. Loss of *APM1* function mutants show embryo lethality and primary root growth arrest 5 days after germination [50]. These phenotypes can be attributed to the premature determinacy of the root meristem from the collapse of the quiescent center (QC) and cell cycle arrest, as shown by absence of QC-25-GUS and *CyclinB1;1* expression respectively [50]. The *APM1* promoter sequence has signature sequences indicating that its expression is regulated by the cell cycle, [49] further supporting a role for APM1 in cell cycle progression. *APM1* is also highly expressed in senescing leaves and metaxylem. These two developmental events, senescence and xylem cell maturation , suggests a role for APM1 in programmed cell death either a direct role in apoptosis or a role in recycling of proteins [50]. There might be various other non-proteolytic activities of APM1 which are suggested by seed and seedling phenotypes in lines where the catalytic and substrate binding domains were mutated [49], [50],but these are yet to be discovered.

Meiotic Prophase Aminopeptidase 1 (MPA1)

MEIOTIC PROPHASE AMINOPEPTIDASE 1 (*MPA1*) is the only M1 Arabidopsis member that resides in the prokaryotic clade of the family phylogenetic tree [49]. Unlike other Arabidopsis M1s, *MPA1* has seven different gene models that suggest the possibility of spatio-temporal regulation. MPA1 is a soluble protein (Chapter 2), and an amino acid sequence comparisons of MPA1 with other M1 aminopeptidases indicated that MPA1 lacks the N-terminal hydrophobic and C-terminal protein–protein interaction domains present in Arabidopsis *APM1* [49]. Arabidopsis MPA1 shows 79%similarity to APM1 and 61% similarity to human PSA at the amino acid level [59]. MPA1 was shown to regulate cell cycle progression during meiosis in both female and male gametophytes, and MPA1 is essential for the homologous recombination and synapsis that takes place in prophase I of meiosis I [48]. Thus, the *mpa1* mutants exhibit a combination of defects. Incomplete synapsis occurred 4-fold more frequently in *mpa1* than wild type, and *mpa1* showed a 90% decrease in homologous crossovers, and an absence of chiasmata. Pradillo et al. (2007) examined the chromosomal segregation pattern in *mpa1* and their data demonstrated that chromosomes 2, 4 and 5 in *mpa1* were mis-segregated in anaphase I suggesting that MPA1 might be a necessary component for synaptonemal complex formation [53]. However, spindle formation appears to be normal in *mpa1* mutants [48], unlike the PSA orthologue *pam-1* [59].The *mpa1* mutants are heterozygous because failures in meiotic chromosome segregation cause infertility [48].Loss of *MPA1* function exhibits chromosome non-disjunction that gives rise to aneuploidy in seedlings and adult plants (Chapter 2). *mpa1* mutants also have shorter primary roots and reduced cotyledon

area in 5 day old seedlings compared to wild type seedlings (chapter 2), as well as incomplete seed filling in siliques [48], (Chapter 2). However, *mpa1* primary root growth is similar to wild type in older seedlings (Chapter 2).

MPA1 may have other roles in addition to chromosome segregation in meiosis and mitosis. A proteomic study showed that when Arabidopsis cell cultures were infected with *Pseudomonas syringae,* MPA1 in the extracellular space was increased [64]. Further, MPA1 localization in the apolpast was increased by type-III effectors (TTEs) such as the surface presentation of antigen *(spa)* and Yersinia outer protein (*yop*). However, apoplastic MPA1 was decreased by microbe-associated molecular patterns (MAMPs) and gene-for-gene resistance [64]. The presence of MPA1 in the extracellular space suggests that MPA1 might have a role in basal plant defense or be involved in modification of extracellular peptides. The high abundance of MPA1 in extracellular space following TTE elicitation could also suggest that MPA1 activity might exploited to provide nutrients for pathogens [64].

Cooperation among M1 family members

PSA orthologue *PAM-1* regulates meiosis and embryogenesis in *C. elegans. pam-1* exhibited reduced embryonic viability and fecundity [59] as mentioned above. PAM-1 shares high sequence similarity with its other M1 paralogs. RNAi inhibition of nine functional M1 paralogs to PAM-1 helped to identify three of active M1 paralogs that have roles independent from PAM-1 in promoting gametogenesis and fecundity. However, simultaneous inhibition of *pam-1* and M1 paralogs resulted in synergistic decreases in overall brood sizes and embryonic viability [59]. This suggested that PAM-1

and its three paralogs exhibit similar catalytic activities. Based on overall results from the study, the researchers suggested that there is 1) an overlap or intersection among their respective pathways or 2) a collaborative of compensatory activity within them in relation to regulation of reproductive success in *C. elegans*.

Taking this concept into consideration, I propose an Arabidopsis example to elucidate a collaborative or compensatory activity within plant M1 members in relation to the regulation of the mitotic cell cycle. The *apm1* knock-down mutants exhibit permanent primary root arrest in 5 day old seedlings [50], and *mpa1* knock-down mutant seedlings display temporary primary root growth arrest at 5 days and the wild type phenotype is naturally restored at 7 days (Chapter 2). The third Arabidopsis orthologue *tata box factor 2-like2* (*taf2l2*) mutant seedlings also share shorter primary root phenotype at 5 days similar to its two sister genes. In an attempt to link these data together, I suggest that *APM1*, *MPA1* and *TAF2L2* have identifiable roles because they might have collaborative or compensatory activity with regard to their function in mitotic cell cycle progression.

Future directions

Zinc metallopeptidases constitute a diverse set of peptidases with important roles in cell maintenance, growth and development, and defense. M1 aminopeptidases are widely distributed across kingdoms with approximately 55 different enzymes are predicted in Archaea, Bacteria and Eukaryotes. However, most of these putative enzymes have not been characterized and no information on their cleavage specificity is available. Research in APN/CD13 has emphasized its role in cell growth. Internalization of ligands bound to CD13 suggests that it might function in cell cycle regulation in other cell types

other than monocytoid. PSA orthologues in other species may have roles in cell cycle regulation.

There are still many outstanding questions about the cell cycle regulating genes *APM1* and *MPA1*. How and when these genes regulate mitosis still need to be addressed. Investigating chromosome segregation at cellular level in *mpa1* and *apm1* using fluorescent in situ hybridization might be an excellent method to discover what mitotic stages are affected in those mutants. This would help elucidate the exact roles that *MPA1* and *APM1* play in mitosis.

Unlike *APM1*, *MPA1* has seven gene models (www.ARAPORT.org) and I postulate that each model is expressed under different conditions producing a range of transcripts. In addition, a natural antisense transcript overlaps with *MPA1* (www.ARAPORT.org). This opens a new avenue to study how, when and where *MPA1* is expressed. Glyma08g01921, a homolog of *APM1*, and *MPA1* and *TAF2L2*, was identified in soybean leaf nuclei which indicates that M1 aminopeptidases might have additional nuclear functions, in addition to meiosis and mitosis [65], as TAF2L2 was shown to have nuclear localization [49] Therefore, there is a the need of more research work on M1 metallopeptidases across kingdoms.

Chapter 2: Mutations in *MPA1* cause developmental defects in *Arabidopsis* seedlings

Introduction

Growth and development in plants is dependent on cellular functions such as mitosis and meiosis. M1 metallopeptidases, also known as gluzicins, have two highly conserved signature motifs located in the catalytic domain: a zinc binding motif, HEXXH, and an exopeptidase motif, GXMEN, that are known to be essential for their catalytic activity. M1 peptidases play a variety of roles in multiple physiological processes including protein maturation, protein turnover and regulation of peptide hormone levels. M1 proteases have been shown to have roles in meiosis and mitosis in plants and animals. *MEIOTIC PROPHASE AMINOPEPTIDASE 1* (*MPA1*) encodes an *Arabidopsis thaliana* M1 metalloprotease previously shown to regulate cell cycle progression during prophase I in meiosis I in both female and male gametophytes and essential for homologous recombination. *mpa1* mutants are maintained as heterozygotes as synapsis failures in male and female gametogenesis preclude obtaining homozygous lines [48].

Here, I have shown *MPA1* expression in 5 day old seedlings is moderate expression in columella cells, lateral root cap, epidermis, cortex and quiescent center and guard cells and epidermal cells in cotyledons using a native promoter driving expression of a functional fluorescent protein fusion (Pro*MPA1*: MPA1- YFP). My results indicate that MPA1 is a soluble protein, and it functions in mitosis in a similar way to meiosis.

Further, I analyzed *MPA1* loss-of-function mutants for polyploidy and developmental phenotypes. I isolated and characterized four new *mpa1* alleles. Three significant phenotypes corresponding to development in seedlings and adult plants in Arabidopsis were observed: 1) chromosome non-disjunction in mitotic cells, 2) altered ploidy, and 3) temporary arrest of primary root growth during seedling establishment.

Methods

Plant material and growth conditions

All plants were used in this study were *Arabidopsis thaliana* Columbia-0 (Col-0) ecotype. New alleles of *MPA1* (At1g63770) were isolated: *mpa1-2* (SALK_060566) and *mpa1-3* and (SALK_006826) were obtained from Arabidopsis Biological Resource Center (ABRC), and *mpa1-4* (GK 010E08) and *mpa1-5* (GK 609B12) were obtained from Nottingham Arabidopsis Stock Centre (NASC). Each line was backcrossed twice. All the plants were grown in growth chambers. Surface sterilized seeds were pated on 1/4 Murashige and Skoog medium (RPI Corp.) containing 0.5% sucrose (w/v) and 0.8% agar (w/v), pH 5.5, stratified at 4 °C for 2 d and placed in growth chambers at 22 °C for 24 h at 100 μmol m^{-2} s^{-1} light for seedling analyses. Seeds were sowed on soil and grown at 22 °C at 100 μmol m^{-2} s^{-1} light (16 h light/8 h darkness) in growth chamber for mature plant analyses.

Genotyping

T-DNA insertion lines, mpa1-2 (SALK_060566), mpa1-3 and (SALK_006826), mpa1-4 (GK 010E08) and mpa1-5 (GK 609B12) were genotyped using primers from SALK T-

DNA and GabiKat primer designing tools, respectively. *mpa1-2*, *mpa1-3*, *mpa1-4* and *mpa1-5* are knockdown mutants which are positioned in 23660120, 23660282, 23658354 and 23658551 respectively in the gene. *mpa1-2* has the insertion in the 20th intron, *mpa1-3* in the 20th exon, *mpa1-4* is in the 27th intron and *mpa1-5* is in the 26th intron.
The primers used to genotype *mpa1-2* were SALK_060566_LP: CAT TCT CTG CTC TGT TCT CGC, and *mpa1-3* SALK_006826_LP: TTT TCC TCT CTC TGG CAG ATG, SALK_006826_RP: CAT TCT CTG CTC TGT TCT CGC and LBb1.3: ATT TTG CCG ATT TCG GAA C. Primers used to genotype *mpa1-4* were GK 010E08 F: GGA AAT ATT GAA CAC AGA GGC TCA, GK 010E08 R: CTA TCC CAG AAC CCT GGT AAA AC, and *mpa1-5* GK 609B12 F: GAC ATT ATC ATT TCC AAT TGT GCC, GK 609B12 R: TAG CCA AAG CAA TAA CACT ACC TG with GK_T-DNA ATA ATA ACG CTG CGG ACA TCT ACA TTT T.

Growth and development related Phenotyping

Seedling and adult plants were photographed and the images were analyzed using ImageJ. Ages of plants are indicated in the figure legends. Cotyledon area of seedlings (5 days after germination) was measured for each line, and the sample size was 15 (n=15) and three replicates were conducted. Primary root length was measured in cm with sample size of 15 with three replicates. For the seed filling count experiment, siliques 5 days after anthesis were fixed in fixative (50% methanol in 10% acetic acid, v/v) for 48 hours at 4 ^{0}C and subjected to an overnight treatment with 1% SDS (w/v) in 0.2 N NaOH (v/v) [66].

Cloning and construction of transgenic lines

Genomic DNA was isolated from rosette leaves using Cetyltrimethylammonium bromide (CTAB) method [67]. The promoter region (2.5 kb upstream from the ATG coding region start site) was amplified using promoter specific primers with their respective restriction sites SacI and XhoI. ProMPA1-SacI: CTGATAgagctcACT ATT GCA TGT GCA TAG ACT TGT and ProMPA1-XhoI: ATGCTActcgagTTC TAA AAA TCC CTA AAG CAA CAA T (restriction site sequences are in lowercase). pUBCYFP-dest Gateway vectors [68] were digested with SacI and XhoI followed by ligation with the *MPA1* promoter (2.5 kb). *MPA1* cDNA (U17812) was obtained from ABRC, PCR amplified and ligated into the modified pUBCYFP vector to develop the construct *MPA1*pro:*MPA1*-YFP (Gateway System (Invitrogen). *MPA1* cDNA (3.2 kb) and *MPA1* promoter (2.5 kb) were inserted into modified pUBCYFP vector using TOPO cloning to make the vector *MPA1*pro: *MPA1*- YFP. Transformation of *Arabidopsis thaliana* with *Agrobacterium tumefasciens* (GV3101) was performed using floral dip as described in Bent et al. (1998) [69].

The overexpression construct pH7CWG2.0-35S promoter-MPA1-CFP used in the experiments was made by Xiping Liu. The *MPA1* cDNA from U17812 was amplified using the primers *MPA1* Sac I F 5’ gagctcATG CAC CTA AAG AAA TAT TTC TCA A-3’ and *MPA1* Kpn I R: 5’ ggtaccTCA AGC AGC CAA ACT CTT GGA G -3’., and inserted into the pGBGWG containing CFP tag to make the vector *35S*pro:MPA1-CFP.

Complementation

The *mpa1-2* loss-of- function mutant was transformed with Pro*MPA1*:MPA1 cDNA. Transformed plants were genotyped using cDNA specific primers to confirm the transformation. Primers used for genotypic confirmation of complementation were:

F primer sequence: 5' TCT CGT GCT CCT GTT CCT GTT AGA AG 3'

R primer sequence: 5' CCT GTC CAA TTG TGA AAG TAC TCA TGA CC 3'

Confocal microscopy

Pro*MPA1*:MPA1-YFP subcellular localization in *Arabidopsis thaliana* seedlings were visualized using Ziess LSM 710 spectral laser scanning confocal microscope (Zeiss.com) using 20X lens or a 40X water immersion lens and pixel dwell time of 0.01 ms, pinhole 90 µm. For YFP acquisition, 514 nm (5%) excitation and 519- to 560-nm emission were used, and the master gain was always set to less than 880, with a digital gain of 1.5. For 35Spro:CENH3-GFP [70] the emission was 488 nm (4.3%), emission, digital gain 1.0, pinhole 38 µm, and the master gain. Z-stack images were collected and analyzed using the 3D visualization option. The florescence intensity was analyzed and quantitated using ZEN Lite 2012. All of the images were taken under the same conditions.

Polyploidy and flow cytometry

Ploidy determination in Arabidopsis cotyledons and rosette leaves was performed at the Flow Cytometry Core at the University of Maryland. The cotyledons or the fifth leaf of the rosette were finely chopped separately in 1 ml of LBO1 buffer (15 mM Tris, 2 mM Na2EDTA, 0.5 mM spermine tetrahydrochloride, 80 mM KCl, 20 mM NaCl, 0.1% Triton

X-100 (vol/vol). The samples were adjusted to pH 7.5 with 1 M NaOH, filtered through 30 µm nylon mesh to obtain 1 ml of final volume. Five µl of RNase (50 mg ml^{-1}) and 50 µl of propidium iodide (50 mg ml^{-1}) were added to the filtrate [71]. 50 cotyledons were used per sample, and 3 mature rosette leaves per sample. Flow cytometry was performed were taken immediately after sample preparation.

CENH3-GFP visual marker for ploidy determination in *mpa1* mutants

mpa1-2 and *mpa1-4* mutants were crossed with a Pro35S:CENH3-GFP marker line [70], and 5-day old mutant seedling roots were imaged. The number of GFP-fluorescent centromeric signals were counted at the two ends in 80 dividing root cells of each line. The data were analyzed using χ2test at a 5% significance level in Excel.

Fluorescence in Situ Hybridization (FISH)

Tissue preparation and chromosome squashes were conducted using 5-day old Col-0 and *mpa1-2* seedlings as described in Walling et al, (2005) [72], Ross et al, (1996) [1] and Pan et al, (1992) [73]. Seeds were sowen on plates and stratified for 48-72 h and move to light, at room temperature. At 2.5 days, seedlings were transferred to filter paper with 1.25 mM hydroxyurea for 18 hrs to synchronize the cell cycle. Then they were rinsed in ¼ MS pH 5.5 3 times and transferred to fresh filter paper. Plants were grown in ¼ MS on filter paper for 4-5 h. Seedlings were transferred to 2 mM 8-hydroxyquinolein at room temperature in the dark to arrest cells in metaphase. Seedlings were fixed 3 ethanol: 1 acetic acid (v/v) (Carnoy's solution) and placed at -20 degrees C (freezer) for 2-3 days before use.

Roots were washed three times with ddH2O to remove fixative and then they were cleared with 45% acetic acid (v/v) 8-10 minutes. Roots were stained with 1% aceto-orcein for contrast. Seedlings were placed on a slide in a drop of 45% acetic acid and covered with a square cover slip. The root tip was crushed with even and gentle pressure on the cover slip using a dull pencil tip to spread the tissue out. After the squash, the slide was gently heated over a flame and checked under the light microscope to verify the success for the squash. The primers used for 180 bp repeats probe design: pAL1_FP 5'-CAC CCA TAT TCG ACT CCA AAA CAC TAA CC-3' and pAL1_RP 5'-AGA AGA TAC AAA GCC AAA GAC TCA T 3' in TOPO cloning vector (www.thermofisher.com). The Thermo-Fisher Scientific nick translation kit was used for probe preparation, and the Thermo-Fisher Scientific FISH protocol was used for the hybridization with modifications of Jackson (1991), Lincoln et al., (1994) [74] and Coen et al. (1990) [75].

Transcription analysis and gene expression

RNA was extracted from 5-day old seedlings using an RNeasy Plant Mini Kit following manufacturer's instructions (Zymo Research). Extracted RNA was used to synthesize cDNA using Superscript transcriptase III (Thermo-Fisher Scientific). Quantitative real-time PCR (qPCR) was performed using SYBR Green on a CFX96 Touch Real-Time PCR Detection System (Bio-Rad). Samples were placed in 96-well optical reaction plates using the following program: 5 min to 95 °C followed by 40 cycles of denaturation for 10 s at 95 °C and annealing–extension for 30 s at 60 °C. The gene specific primers used to quantify *MPA1* expression levels were N-terminal primers: RTMPA1_F: ATG GCT

CGG TTG ATA ATT CCT TGT, RTMPA1_R: ATC AAC AGA ATG GGG TAG AAA CCG AT, RTMPA1_2_F: CGT ATG GTG TCT GCC TTT TCG AGG and RTMPA1_2_R: AGC CAA ACT CTT GGA GGC AAT, C-terminal primers: RT-PCR_F 2 CTT GGC TAG ACC TTG ACG GGT TT, RT-PCR _R 2 GGG TGA CAT TGT TGT CCA GTT A. The primers used for the *PROTEIN PHOSPHATASE 2A* (*PP2A;* At1g69960) as the reference gene were PP2A FOR: TCG TGG TGC AGG CTA CAC TTT C and PP2A REV: TCA GAG AGA GTC CAT TGG TGT GG.All quantitative RT-PCR experiments were performed with three technical and biological replicates. Data were analyzed using CFX Manager software (Bio- Rad). The values presented in the graphs represent means ± SE of three biological and three technical replicates for each biological replicate.

Statistical Analysis

Data were analyzed one-way ANOVA was performed using SPSS (Statistical Package for the Social Sciences) followed Tukey's post-hoc analysis. Statistically significant differences were defined as $P < 0.05$. Values in graphs were presented as means and standard deviation of three replicates. Microsoft Excel 2017 (Microsoft Corporation) data management, statistical analysis, and graph generation.

Results

MPA1 is expressed in seedlings

According to microarray and RNAseq data presented in the Bio-Analytic Resource for Plant Biology (BAR) and Transcriptome Variation Analysis (TRAVA) databases, *MPA1* is mildly expressed in most parts of adult plant and seedlings (http://bar.utoronto.ca; http://travadb.org). *MPA1* is expressed at intermediate levels in seedling primary root, guard cells in cotyledons and true leaves. It is highly expressed in dry seeds, imbibed seeds, shoot and root apical meristems including quiescent center and senescent leaves. This suggested that *MPA1* is expressed in regions that have rapidly dividing cells. RNAseq data also show that *MPA1* is abundantly expressed in M phase and S phase of the cell cycle (www.cyclebase.org). These expression data support my hypothesis on *MPA1* regulates the mitotic cell cycle.

MPA1 expression patterns were analyzed in 5-day old seedlings using a *MPA1* native promoter to drive an *MPA1* cDNA fusion with yellow fluorescent protein tag (Pro*MPA1*:*MPA1*-YFP). Pro*MPA1*: MPA1-YFP signals were observed throughout the seedling, with highly signals in the primary root, shoot meristem and cotyledon guard cells and subsidiary cells. MPA1 signals were also strong in the root meristem (Figure 2A). Pro*MPA1*: MPA1-YFP signals are consistent with the published *MPA1* expression data. This data strongly support that *MPA1* is expressed in tissues where a rapid and continuous cell division takes place and MPA1 might play an important role in seedling development and establishment. Further, confocal microscopy also showed that *MPA1*-

YFP is cytosolic (Figure 2D). The autofluorescence images of Col-0 are shown in Supplementary Figure 1.

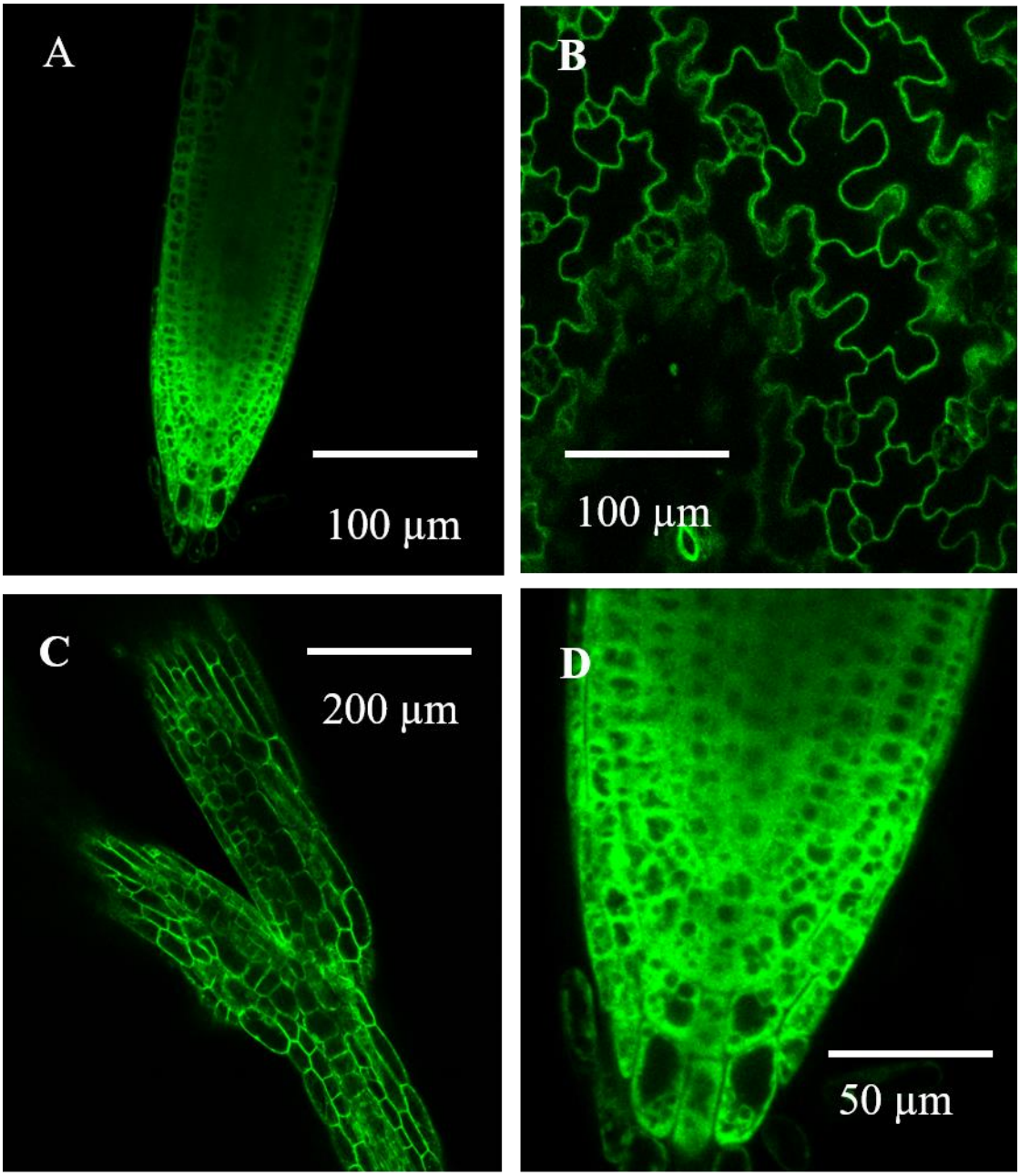

Figure 2. Spatial and temporal expression of *MPA1* in seedlings. *MPA1*pro:MPA1-YFP signal in 5-day old seedlings. (A) Primary root, (B) Cotyledon, (C) Cotyledonary node, (D) Cytosolic localization of MPA1 in the root. All the images were taken under the same conditions.

Isolation of verification of *MPA1* loss-of-function alleles

The schematic representation of gene map of *MPA1* is shown in Figure 3A, and MPA1 protein structure is presented in Figure 3B. *MPA1* has 28 exons and 27 introns. All four alleles have insertions that are 3' of the catalytic domain. The relative expression of *MPA1* in each line was analyzed by quantitative real-time PCR (qPCR) using primers to exons 1 and 2 or exons 27 and 28. Quantitative real-time PCR (qPCR) showed *MPA1* expression in *mpa1-2, mpa1-3, mpa1-4* and *mpa1-5* were less than 50% compared to wild type using either set of primers ($P < 0.05$; Figure 3C and Figure 3D).

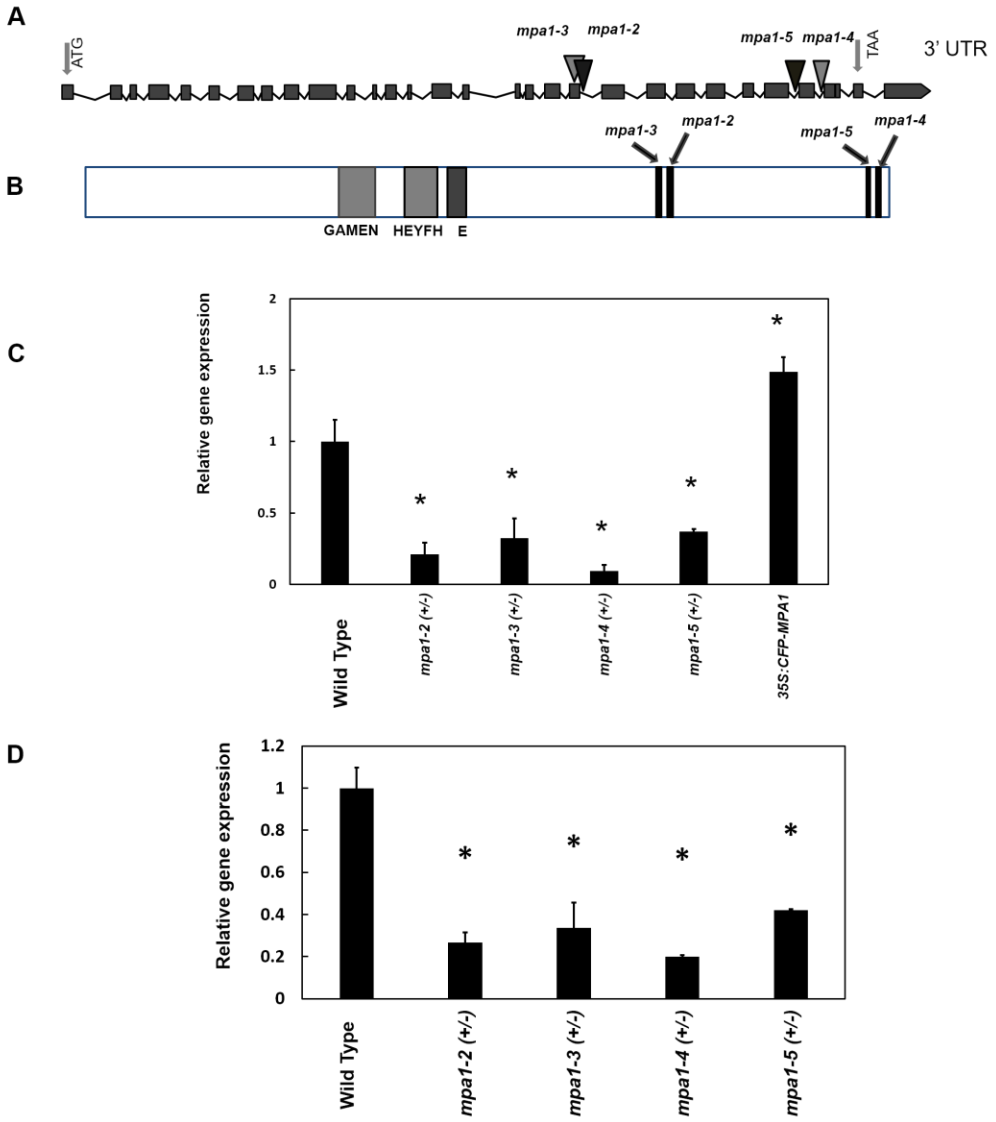

Figure 3. Gene map, protein map and relative gene expression of *MPA1*. (A) Map of *MPA1* (At1g63770) gene structure and mutation sites, with the start (ATG) codon, exons (boxes), introns (lines), and the position of the mutational sites (T-DNA insertions, triangles). (B) Graphical representation the of MPA1 protein. The catalytic motif (HEYFH) and exopeptidase domain (GAMEN) are indicated by gray boxes and the locations of mutational sites are indicated in relation to signature domains. Mutation sites are indicated by arrows. (C) Relative gene expression of *MPA1* in *mpa1* mutants using N-terminal primers. (D) Relative gene expression of *MPA1* in *mpa1* mutants using C-terminal primers. RNA was extracted from 5-day old seedlings of wild type and *mpa1* mutants and qRT-PCR was conducted with *PP2A* as the reference gene. Data represent means ± SD of three biological and three technical replicates for each biological replicate. $P < 0.05$ compared to wild type; ANOVA followed Tukey's post-hoc analysis.

MPA1 loss-of-function mutants show altered phenotypes

Primary root length of 5-day old *MPA1* loss-of-function seedlings was significantly shorter compared to Col-0 ($P < 0.05$; Figure 4A). However at 7 days after germination, the primary roots of all alleles were similar in length to wild type ($P > 0.05$; Supplementary Figure 2A). Cotyledon area was significantly smaller in *mpa1* alleles compared to Col-0 in 5-day old seedlings (Figure 4), but cotyledon area in 7-day old seedlings were highly variable in size with individual *mpa1* seedlings showing cotyledons that were larger, smaller or similar in size to Col-0 cotyledons. When *mpa1-2* was transformed with Pro*MPA1*:MPA1 cDNA, the *mpa1-2* reduced root length at 5 days and cotyledon area phenotypes were complemented ($P > 0.05$; Supplementary Figure 3). This indicates that the temporary arrest in primary growth and smaller cotyledon size at 5 days were due to the lesion in *MPA1*.

I further investigated other root- and shoot-related phenotypes in *mpa1* seedlings. Since *mpa1* seedlings showed reduced primary root elongation at 5 days, I examined the root meristem size, the length between quiescent center to the beginning of elongation zone. However, the root meristem size in 5-day old *mpa1* seedlings was not statistically different from wild type ($P > 0.05$; Supplementary Figure 4). Further, the lateral root number in 10-day old *mpa1* showed no statistical difference ($P > 0.05$; Supplementary Figure 5). *MPA1* is highly expressed in dry seeds and imbibed seeds according to microarray and RNAseq data. Therefore, I examined the seed germination rate in *mpa1*,

but no statistically significant difference was observed in number of *mpa1* seeds germinated in each day compared to wild type ($P < 0.05$; Supplementary Figure 6).

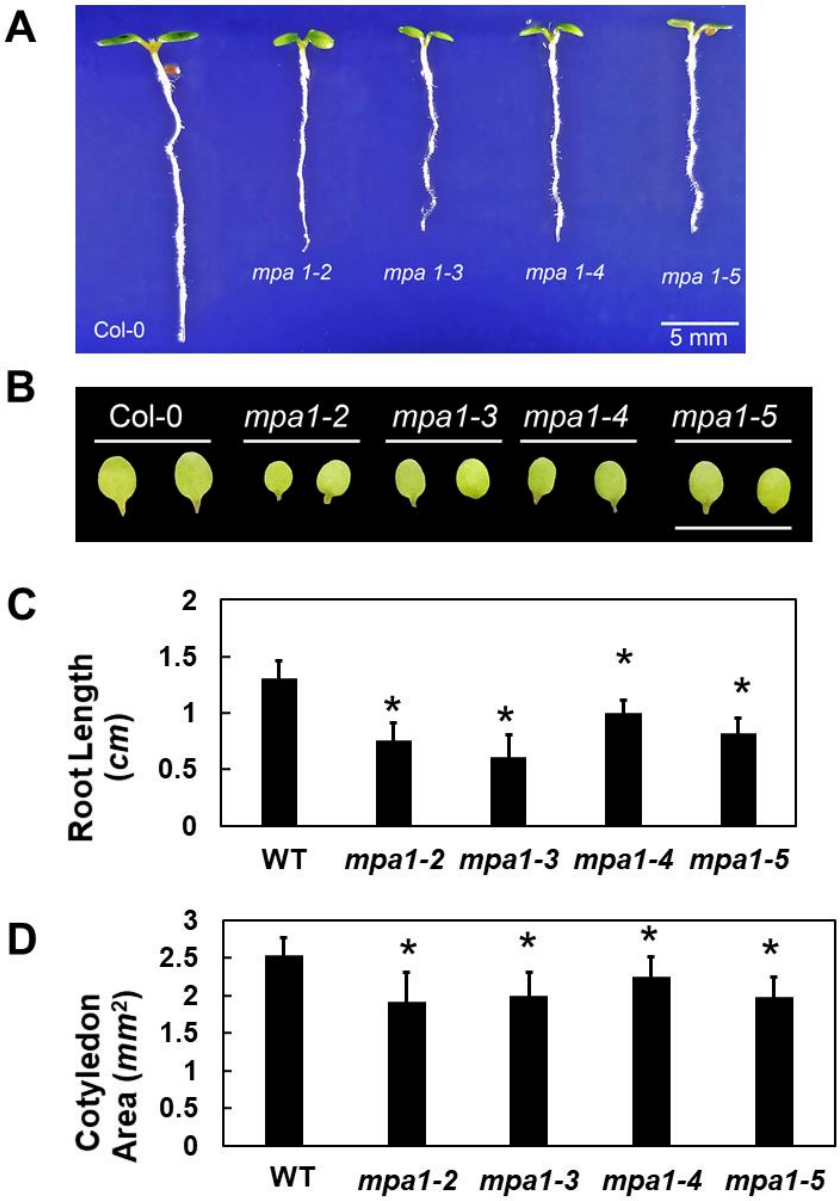

Figure 4. Five–day old *MPA1* loss-of-function alleles have altered phenotypes. (A) Primary root length, (B) quantification of primary root lengths in (A), (C) cotyledon area, (D) quantification of cotyledon area in (C). Data are means and standard deviations from three independent experiments (n=15). * $P < 0.05$ compared to wild type; ANOVA followed Tukey's post-hoc analysis.

Reduced seed yield in *mpa1*

According to Sanchez et al. (2004), *mpa1* mutants showed reduced fertility by producing shorter siliques with fewer seeds compared to Col-0 plants. Therefore, *mpa1-2, mpa1-3, mpa1-4* and *mpa1-4* siliques were investigated for seed filling and number of seeds per silique (Figure 5A). The number of seeds per silique in Col-0 ranged from 39 to 55 and the majority siliques had 39-40 seeds (Figure 5B). Seed number in *mpa1* siliques varied from 27 to 34, but the majority had 29-30 seeds per silique. The number of missing seeds in *mpa1* mutants compared to Col-0 was approximately 10-11. Incompletely filled *mpa1* siliques may be attributed to defects in male and female meiosis. Reduced silique size and silique filling also occurs in the M1 aminopeptidase *APM1* loss-of-function mutants; however, this is due to defects during gametogenesis [2], [50].

Table 1 shows segregation analysis of the loss of *MPA1* lines that were backcrossed twice and confirmed by genotyping. Adult rosette leaves were used to extract gDNA. The expected phenotypic ratio from normal Mendelian inheritance is 3 wild type: 1 mutant, and the expected genotypic segregation ratio is 1 *MPA1/MPA1*: 2 *MPA1/mpa1*: 1 *mpa1/mpa1*. However, I inferred from a previous report that *mpa1* mutants need to be maintained as heterozygotes [48], the expected genotypic ratio is 1 *MPA1/MPA1*: 2 *MPA1/mpa1,* and I tested this hypothesis.

The data were analyzed using $\chi 2$, and the values obtained were smaller than the critical $\chi 2$value (3.841, α=0.05). This indicated that there was no statistically significant difference in expected and observed ratios. Therefore, I conclusively showed as *mpa1* mutants segregate with 1 *MPA1/MPA1: 2 MPA1/mpa1* ratio. Collectively, these results are consistent with the incompletely filled siliques in *mpa1* alleles and that homozygous *mpa1* are not observed due to the meiotic defects previously reported [48].

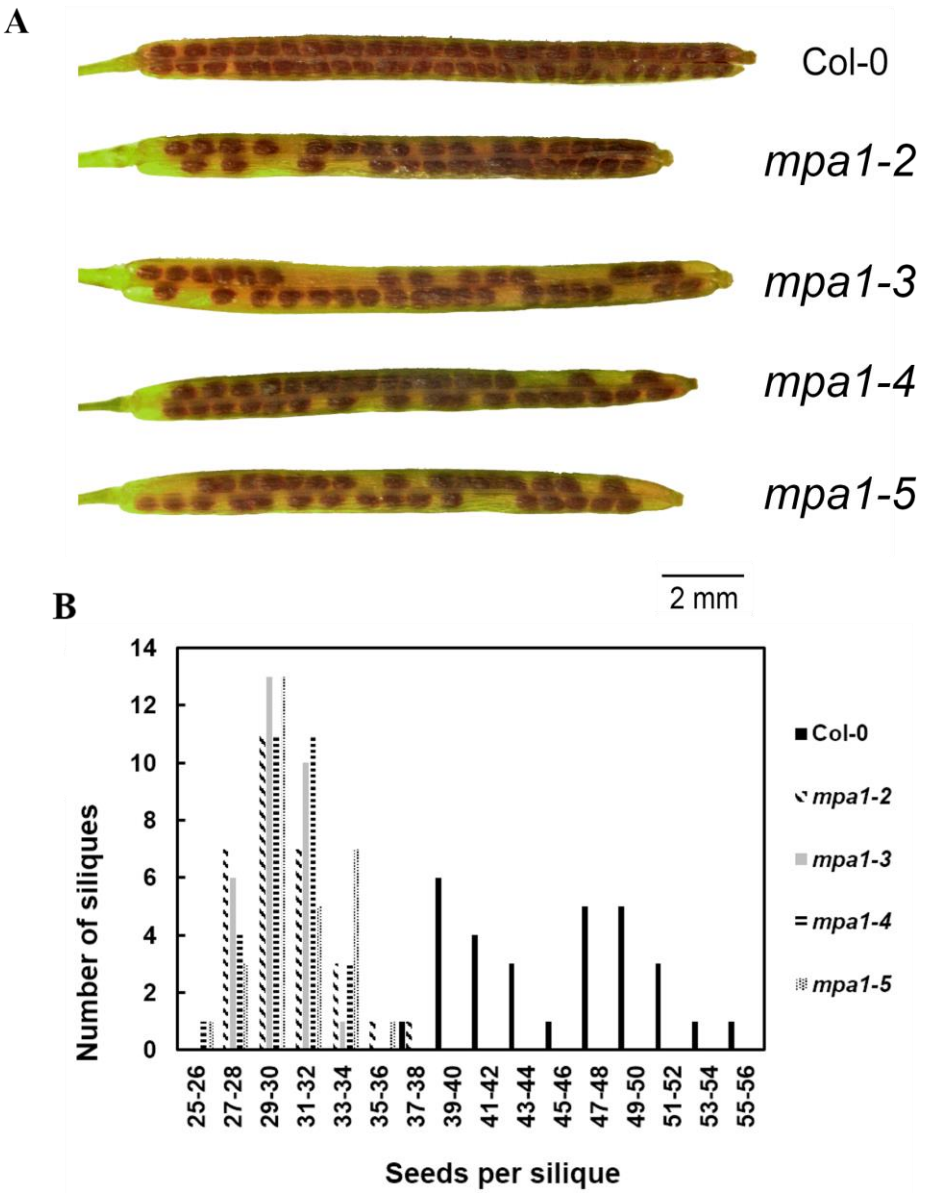

Figure 5. Seed yield is altered in *mpa1*. A Wild type and mpa1 mutant siliques. B. Quantitative classification of seed number in mpa1 and wild type siliques. Three independent experiments were conducted (n=10).

Table 1. Genetic analysis of loss of *mpa1* segregation ratios. *MPA1* loss-of -function mutants were backcrossed twice and then the progeny were genotyped for segregation ratios.

	Progeny		
	Genotype		
	1 BC		$\chi^{2,\,a}$
	Wild type	*mpa1* (+/-)	1:2
Parents			
MPA1/*mpa1-2* x Col-0	12	32	0.727273
MPA1/*mpa1-3* x Col-0	14	33	0.265957
MPA1/*mpa1-4* x Col-0	17	31	0.09375
MPA1/*mpa1-5* x Col-0	20	35	0.227273
	Genotype		
	2 BC		χ^2
	Wild type	*mpa1 (+/-)*	1:2
Parents			
MPA1/*mpa1-2* x Col-0	14	30	0.045455
MPA1/*mpa1-3* x Col-0	11	32	1.162791
MPA1/*mpa1-4* x Col-0	9	26	0.914286
MPA1/*mpa1-5* x Col-0	12	27	0.115385
	Genotype		
	Reciprocal crosses		χ^2
	Wild type	*mpa1 (+/-)*	1:2
Parents			
MPA1/*mpa1-2* x Col-0	14	25	0.115385
Col-0 x MPA1/*mpa1-2*	16	30	0.043478

[a] Probability was calculated using χ2analysis for *mpa1* segregation ratio. [The ratio expected was 1:2 (1 wild type: 2 heterozygotes), df = 1] Critical χ2 values were smaller than 3.841 (α=0.05). The expected ratios for a recessive mutation were observed.

Vegetative and other reproductive phenotypes

I further examined adult *mpa1* plants to determine if they had phenotypes differing from the wild type. Characteristics examined were the number of leaves in a rosette, rosette diameter, inflorescence height and the number of secondary branches. Statistical analysis of number of rosette leaves in *mpa1* plants indicated that there is no significant difference in rosette leaf number or rosette diameter in mutants compared to Col-0 ($P > 0.05$; Supplementary Figure 7, Supplementary Figure 8). Also, no difference was observed in the number of secondary branches or inflorescence height in *mpa1* compared to Col-0 ($P > 0.05$; Supplementary Figure 9, Supplementary Figure 10).

Chromosome segregation analysis

Chromosome segregation is the process by which sister chromatids or chromosomes separate and migrate to daughter cells via mitosis and meiosis. Since *Arabidopsis thaliana* has 10 chromosomes, each mitotic daughter cell is expected to have 10 chromosomes. If chromosome non-disjunction occurs, then an asymmetric distribution of chromosomes will be observed in the two daughter cells. *CENH3* is a centromere-specific histone 3 variant found in the nucleosomes of functional centromeres. The CENH3-GFP reporter allows for *in vivo* chromosome quantification in single cells [70]. To test the hypothesis that MPA1 regulates normal chromosome disjunction during mitosis, *mpa1* alleles were crossed with Pro35S:CENH3-GFP. Dividing root cells in 5-day old Col-0 and *mpa1* seedlings expressing Pro35S:CENH3-GFP were analyzed for fluorescent centromeric dot distributions (Figure 6A). The *mpa1* alleles showed statistically significant differences in asymmetric CENH3-GFP signal distributions compared to wild

type (Table 2). The number of dividing root cells displaying non-disjunction were significantly greater in *mpa1-2* and *mpa1-4* compared to Col-0 Table 2). These results indicate that the chromosomes in *mpa1* somatic cells fail to segregate properly during mitosis, and strongly support the hypothesis of *MPA1* regulates mitosis via chromosome disjunction in a similar way to meiosis. Therefore, *MPA1* has similar roles promoting chromosome disjunction in mitosis and meiosis.

Table 2. Statistical analyses of 35S:CENH3-GFP signals during chromosome segregation. The probability was calculated using χ2 analysis for number of dividing root cells with chromosome non-disjunction in *mpa1*. [The ratio expected was obtained from the number chromosomes displaying disjunction and non-disjunction observed in Col-0 (45:35), df = 1] Critical χ2 values are larger than 3.841 (α=0.05).

	disjunction number	non-disjunction number	χ^2
Col-0	45	35	
mpa1-2	26	54	18.33651
mpa1-4	26	54	18.33651

Ploidy patterns are altered in loss of *MPA1* alleles

The C-values in cotyledons and mature leaves were quantified using flow cytometry to determine if *MPA1* gain- and loss-of-function lines exhibit variation in ploidy composition compared to Col-0. The C-value is the nuclear DNA content, in other words, the C-value is the genome size in unreduced gametes or somatic cells [76], and higher C-values indicate greater DNA content. The baseline C-values for diploid somatic cells is 2C, and cellular ploidy levels can be increased by a number of mechanisms such as aneuploidy and endoreduplication. The C-values were analyzed for each line (Figure 6B and 6C). The 4C value was determined to be most elucidative for comparison of *MPA1* gain- and loss-of-function lines to evaluate the role of MPA1 regulating ploidy levels.

Compared to wild type, the cotyledons of *mpa1-2*, *mpa1-3* and *mpa1-4* showed a 33% reduction in 4C nuclei (Figure 6B). However, cotyledons from *mpa1-5* and the *MPA1* overexpression line (35S:MPA1-CFP) had twice as many 4C nuclei as wild type (Figure 6B). This indicates that there is a decrease in 4C ploidy level in *mpa1-2*, *mpa1-3* and *mpa1-4* alleles, and an increase in *mpa1-5* and overexpression line. The altered ploidy levels in the cotyledons may account for the reduced cotyledons area observed in 5-day old seedlings (Figure 4). These data suggest that MPA1 acts as a negative regulator of ploidy in cotyledons.

In contrast to cotyledons, there was little variation observed in the rosette leaf ploidy composition in *mpa1-5* and *MPA1* overexpression lines compared to wild type (Figure 6C), which is consistent with rosette phenotypes observed (Supplementary Figure 7, Supplementary Figure 8). However, *mpa1-2* and *mpa1-3* had three times and *mpa1-4* had 30% more 4C nuclei as wild type (Figure 6C). This suggests that MPA1 may have different roles in embryonic and mature tissues.

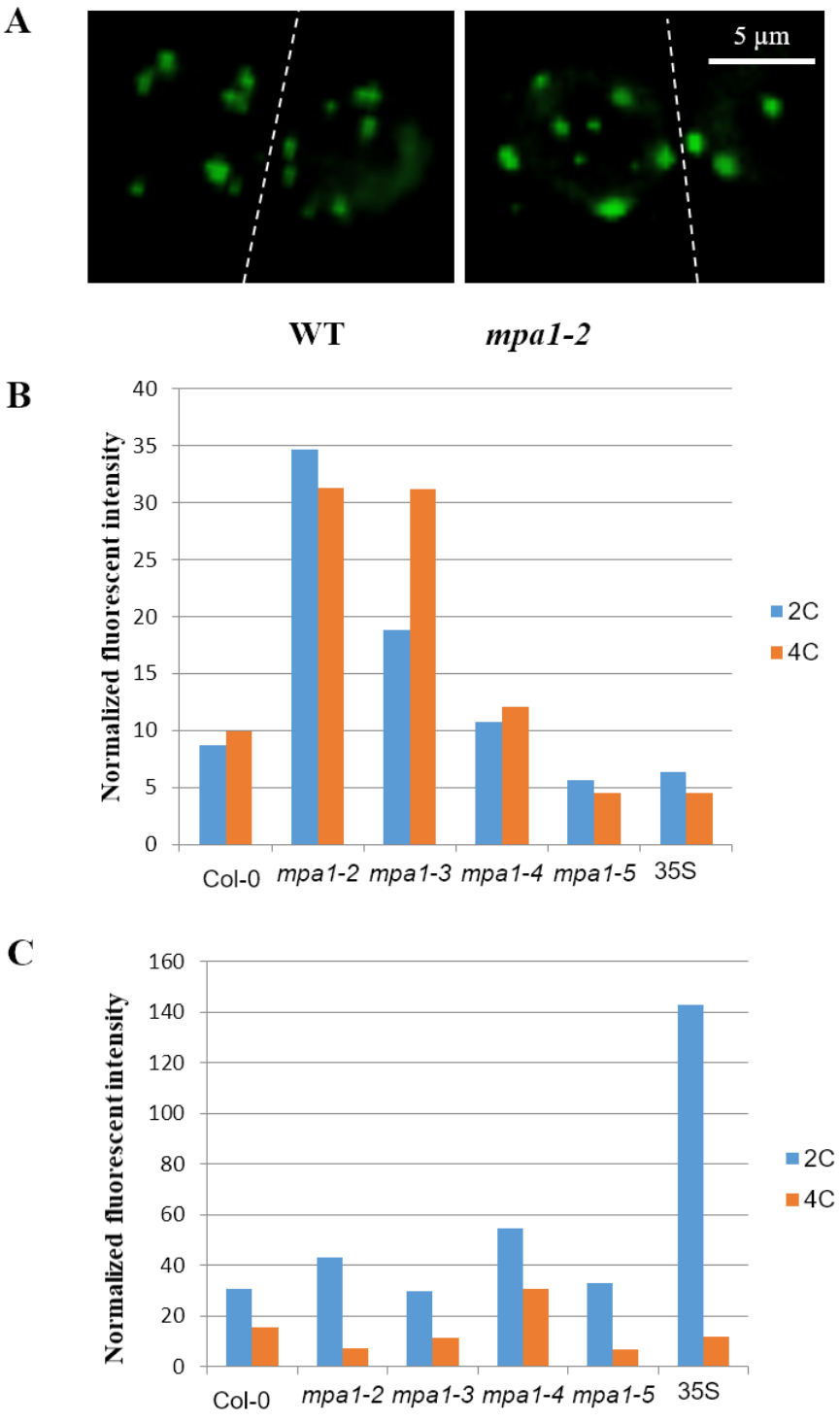

Figure 6. Defects in mitosis cause variation in ploidy levels in *mpa1*. (A) 35S:CENH3-GFP localization in centromeres of *mpa1*, uneven distribution of chromosomes in *mpa1*. The dotted line represent the cell division plane. Flow cytometry of cotyledons (B) and rosette

leaves (C). Altered ploidy composition observed in *mpa1*. The normalized fluorescent intensity is represented by the Y axis.

Discussion

MPA1 is expressed in dividing cells

Pro*MPA1*: MPA1-YFP localization in primary root of 5-day old seedlings suggest MPA1 has a role in seedling development and establishment in *Arabidopsis thaliana* (Figure 2). Strong MPA1 localization signals are observed in the meristematic regions of root and shoot where continuous and rapid cell division occurs (Figure 2). This supports the hypothesis that *MPA1* might regulate mitosis in Arabidopsis; however, MPA1 does not regulate the rate of mitosis, since no changes in meristem size were observed (Supplementary Figure 4). Pro*MPA1*: MPA1-YFP signals are observed throughout the root and in cotyledons epidermal, guard and subsidiary cells in cotyledons. Since loss-function lines show temporary primary root growth arrest and reduced cotyledon area at 5 days (Figure 4), this indicates that MPA1 may have a role in cell expansion in roots and cotyledons.

All post-embryonic organs, including leaves, flowers and axillary meristems, are initiated in the shoot apical meristem. Even though there are differences in ploidy levels (Figure 6), this difference does not seem to translate into obvious phenotypes in adult plants. Interestingly, *MPA1* expression is observed in reproductive structures and in vegetative dividing cells which indicates *MPA1* might play a role in regulating both the meiotic and mitotic cell cycle.

MPA1 is important for seedling establishment

MPA1 appears to be required for primary root meristem maintenance during early seedling development. Five-day old heterozygous knock-down *mpa1* seedlings display shorter primary roots compared to wild type. However, a permanent primary root growth arrest was not observed in *mpa1* knock-downs as in *apm1* [50], and the arrest in *mpa1* alleles described here is temporary. *APM1* and *MPA1* shares 81% amino acid similarity and 76% nucleic acid similarity with *APM1* (www.ncbi.nlm.nih.gov/BLAST). Gene homology is useful in predicting gene function. High sequence similarity outside of the conserved motifs between MPA1 and APM1 suggest sharing similar functions. APM1 has an effect on mitotic cell cycle progression, and I hypothesized that MPA1 might also have a role in regulating cell cycle progression. However, after 5 days, *mpa1* roots grow continuously and ultimately form lateral roots like wild type. Intriguingly, seven days after germination, no discernable difference is observed in root lengths between Col-0 and *mpa1*. Therefore, MPA1 activity promotes primary root elongation from germination through 5 days after germination. Nonetheless, after seven days, the MPA1 activity might not be critical for root growth; thus, seedlings tend to grow continuously. Severe defects in *mpa1* produce unviable gametes, thus reduced seed yield is observed.

The *mpa1-1* allele studied in Sanchez et al. (2004) [48] was a knockout mutant which has the T-DNA insertion in 3' UTR [48], while the *mpa1-2, mpa1-3, mpa1-4* and *mpa1-5* are knockdown mutants have T-DNA insertions in an exon and introns in the C-terminal half of the gene, which may produce partially catalytically active proteins. I tried to obtain the *mpa1-1* allele, but it is no longer available. The *mpa1-1* null allele was not reported to

display arrested primary root phenotype ([48]), but all four new *mpa1* alleles show a temporary primary root arrest at 5 days. *mpa1-2,* The smaller silique size phenotype observed in *mpa1-1* was not observed in new *mpa1* alleles [48]. Therefore, I hypothesize that might be due to the location of the insertional sites in *mpa1-1* reduced the severity of the mutation. I hypothesize that mRNA stability is altered in *mpa1-1* since the insertion is in the 3' untranslated region.

The *mpa1* mutants are haplo-insufficient since they must be maintained as heterozygotes (Table 2). While relative gene expression data show depressed steady-state levels of mRNA, (Figure 3), the cDNA complements the mutants. Therefore, I hypothesize that RNA synthesis was disrupted by a RNA silencing mechanism that induces the degradation of mRNA. mRNA stability influences gene expression in all organisms. The balance between mRNA synthesis and degradation is the key determinant factor of mRNA stability. Down-regulation of genes adversely affects protein stability. Small interfering RNA (siRNA), and microRNA (miRNA) bind to complementary targets and regulate post transcriptional gene expression [77], and affect mRNA stability and subsequent protein synthesis.

In meiosis, prophase I homologous chromosomes remain bound together by crossovers and synaptonemal complexes. The correct positioning of homologous chromosomes in metaphase I and proper segregation in anaphase I are supported by chiasmata formation and sister chromatic cohesion. In *mpa1* the segregation of homologous univalent of chromosome 2, 4 and 5 in anaphase I is not random compared to other meiotic mutants such as *asy1 (asynaptic),* and *spo11-1-3 (sporulation defective)* [53]. Data from this work suggested that there is a chromosome segregation system which is facilitated by

synaptonemal complex formation, that eventually regulate disjunction of homologous chromosomes in anaphase I [53]. However, Pradillo et al. (2007) observed *mpa1* reaching the full synapsis which contradicts what Sanchez et al. (2004) observed in their work as *mpa1* show de-synapsis in prophase I. Nonetheless, MPA1 functions in chromosome disjunction in meiosis.

Surprisingly, a natural anti-sense RNA in *Arabidopsis thaliana* (AT1G08633) overlaps with the first two exons of the *MPA1* gene (www.araport.org). Antisense RNA is involved in post-transcriptional gene silencing by forming a duplex with the target mRNA to promote its degradation or inhibit the translation [78]. According to RNAseq expression data, AT1G8633 is highly expressed in 7-day, 10-day and 11-day old Arabidopsis seedlings. Based on this novel data, I hypothesize that after 5 days, MPA1 activity may be transcriptionally controlled by the natural antisense RNA. *MPA1* expression might be detrimental to the seedling establishment after 5 days, hence the natural antisense RNA might down regulate the *MPA1* expression that eventually promotes continuous primary root elongation. In addition to that, MPA1 has seven gene models that produce transcripts different form one another. Therefore, MPA1 ultimately encodes seven unique proteins. Thus we can hypothesize that spatial and temporal alternate splicing of the gene models might be regulated by the natural antisense RNA.

MPA1 affects ploidy

Polyploidy is genome doubling or whole genome duplication in an organism [79] and aneuploidy is a gain or loss of an individual chromosome or a segment of a chromosome [80].

The flow cytometry data and 35S:CENH3-GFP data support the hypothesis that *mpa1* alleles show aneuploidy in mitotic cells due to chromosome non-disjunction in anaphase (Figure 6A, B and Table 2). There are three ways that chromosome non-disjunction occurs: Homologous chromosomes mis-segregate in anaphase I, meiosis I, sister chromatids fails to separate properly into daughter cells during meiosis II, and mis-segregation of sister chromatids in anaphase in mitosis. Non-disjunction results in daughter cells with abnormal chromosome numbers, known as aneuploidy. Endoreduplication cycles also results in polyploidy [81]. However, polyploidy does not always produce expanded or enlarged cells. The flow cytometry data of 5-day old cotyledons indicated that *MPA1* acts as a negative regulator of ploidy as *mpa1-2, mpa1-3* and *mpa1-4* display a decrease in 4C level compared to Col-0 and overexpression line. These data support the differences observed in cotyledon area among the *mpa1* alleles compared to wild type (Figure 4B, D).

However, the altered ploidy showed no or subtle phenotypes in the adult plants, such as rosette size (Supplementary Figure 7, Supplementary Figure 8, Supplementary Figure 9 and Supplementary Figure 10). Ploidy composition in *Arabidopsis* leaves ranges from 2C to 32C, as a result of the number of endoreduplication cycles. Putting all the flow cytometry data together, variation in ploidy composition among *mpa1* alleles suggests that perhaps different transcripts of *MPA1* may be expressed at different growth stages of the plant development.

MPA1 acts as a negative regulator of polyploidy, but it does not seem to affect mitosis because no statistically significant difference is observed in root meristem size in *mpa1*. Cyclins regulate cell cycle by activating cycling dependent kinases (CDKs).

Pro*cyclinB1*;1:GUS is marker widely applied in mitotic cell cycle studies in plants. The Pro*cyclinB1*;1:GUS activity was not observed in the root meristematic region of *apm1-1* heterozygotes or homozygotes. The cell division appeared to be halted in *apm1* mutants and that is consistent with the arrested primary root growth phenotype in *apm1* mutants. I suggest that examination of the cell division in *mpa1* root meristem using Pro*cyclinB1;1*-GUS expression is necessary as a continuation of this line of investigation. Fluorescence *in situ* hybridization (FISH) [82] is a technique used for cytogenetic studies to visualize fluorescently labeled chromosomes under the microscope. I attempted arresting mitosis at metaphase using 8-hydroxyquinolein [73], [72] in *mpa1*, but the cells were not sufficiently arrested at metaphase. However, I suggest visualizing chromosome segregation in metaphase and anaphase in roots cells using FISH might provide evidence to strengthen our hypothesis on *MPA1* regulating chromosome disjunction, and identifying the stage(s) where MPA1 acts during meiosis and mitosis.

A possible mechanism for MPA1 catalytic activity is activating and inactivating a separase enzyme. Separase is a protein required at anaphase to cleave the cohesin complex to separate sister chromatids [33], similarly MPA1 appears to also be a component of the chromatid separation machinery. More studies needed to test this hypothesis. As Sanchez et al. [48] hypothesized, the destabilization of RAD51, the RecA homolog in Arabidopsis, and mis-localization of MSH4, the eukaryotic homolog of the *E. coli* MutS mismatch repair protein, may suggest that MPA1 may effect one or more other proteins in the cell cycle regulation process [48]. MPA1 activity might be directly or indirectly important for the MSH4 activity to proceed with later stages of meiotic

progression. This suggests that MPA1 might have a collaborative role with other proteins in governing the meiotic cell cycle in Arabidopsis.

Polyploidy and aneuploidy can be advantageous for plants in numerous ways. It can mask detrimental recessive mutations and allow mutants to ensure their fitness in the environment in which they live. In addition to that, polyploids can evolve new functions that are different from their parents and this can help to improve adaptability of these plants to survive in stressful environments [83].Disadvantages of polyploidy can lead to reduced vigor. An increased number of chromosomes increases the complexity of chromosome pairing and segregation interactions. This can cause abnormalities during both meiosis and mitosis [84][81].

MPA1 is a soluble protein as demonstrated by MPA1-YFP has a cytosolic localization (Figure 2D). Microarray data published in ARAPORT indicate that *MPA1* expression is extremely abundant in dry seeds and imbibed seeds. Seeds accumulate high levels of protein storage bodies or vacuoles to be used as sources of nitrogen and energy for the germinating seedlings [85]. This might suggest MPA1 has a role in nutrient mobilization. An experiment can be conducted to investigate if there are differences in seed storage proteins in the mutant seeds.

Co-expression of genes along with *MPA1* or suppression of *MPA1* by neighboring genes, such as the natural antisense gene AT1G08633, suggest other mechanisms for *mpa1* plants to display these prominent phenotypes. In addition to that, functional proteomics studies of MPA1 would be very beneficial to discover the molecular and biochemical functions of MPA1. Therefore, looking at MPA1 post-translational modifications and

protein-protein interactions might help discover more about MPA1 and other sister M1 aminopeptidases that share similar functions.

Supplementary figures

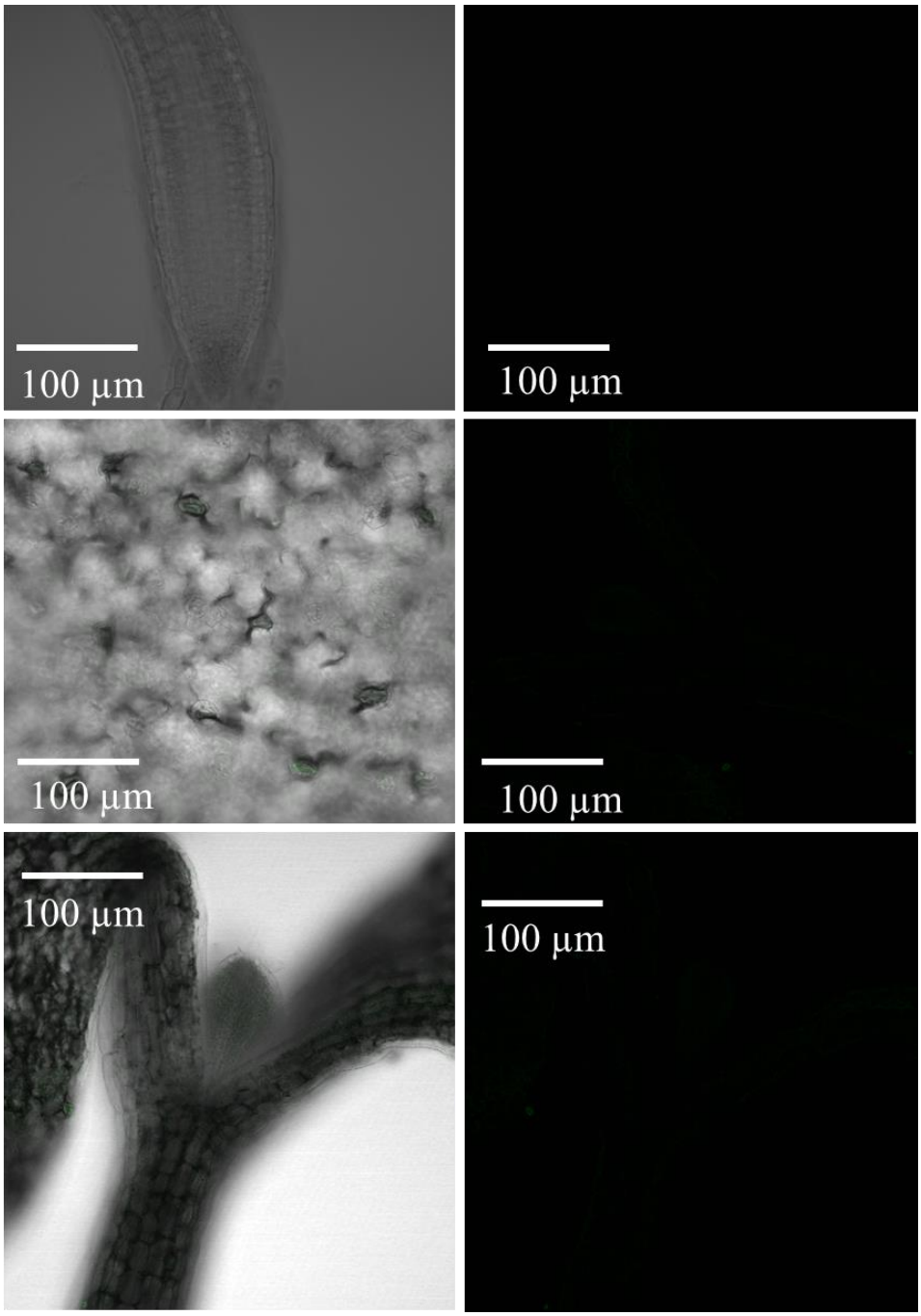

Supplementary Figure 1. Autofluorescence controls of wild type plants corresponding to confocal images in Figure 2. Images were taken on an LSM710 confocal spectral laser scanning microscope. All the images were taken under the same conditions corresponding images in Figure 2

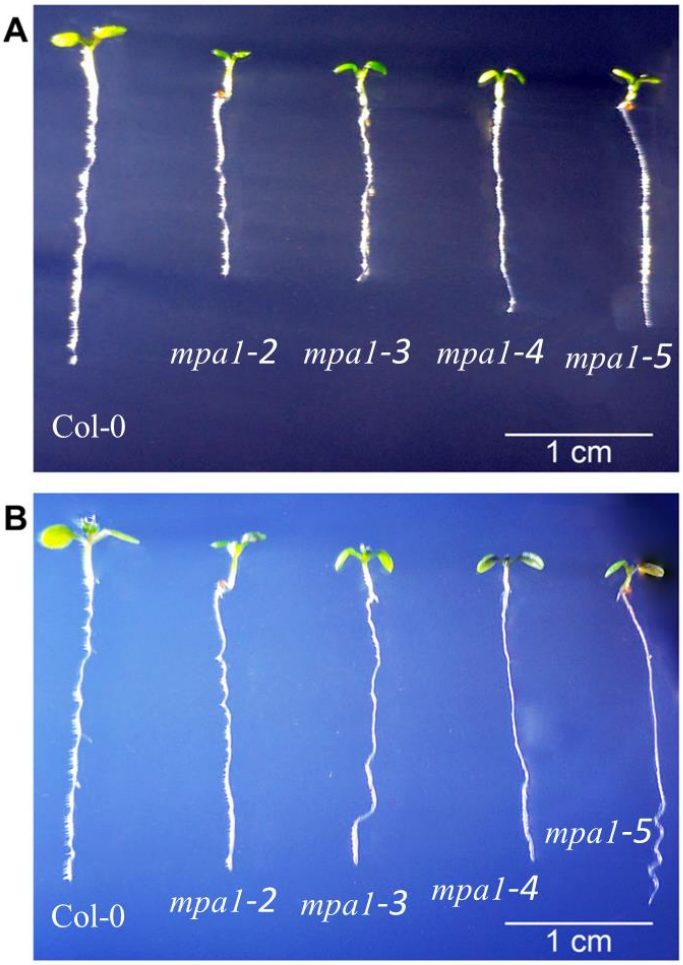

Supplementary Figure 2. Primary root growth comparison of *mpa1* seedlings at 5 days and 7 days.

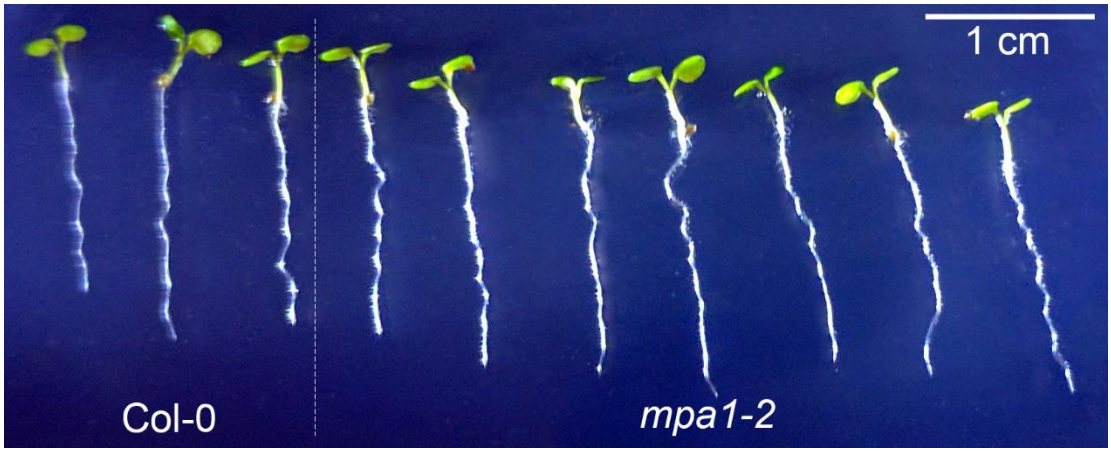

Supplementary Figure 3. Restoration of primary root length in *MPA1pro*:MPA1-YFP complemented 5-day old *mpa1-2* seedlings.

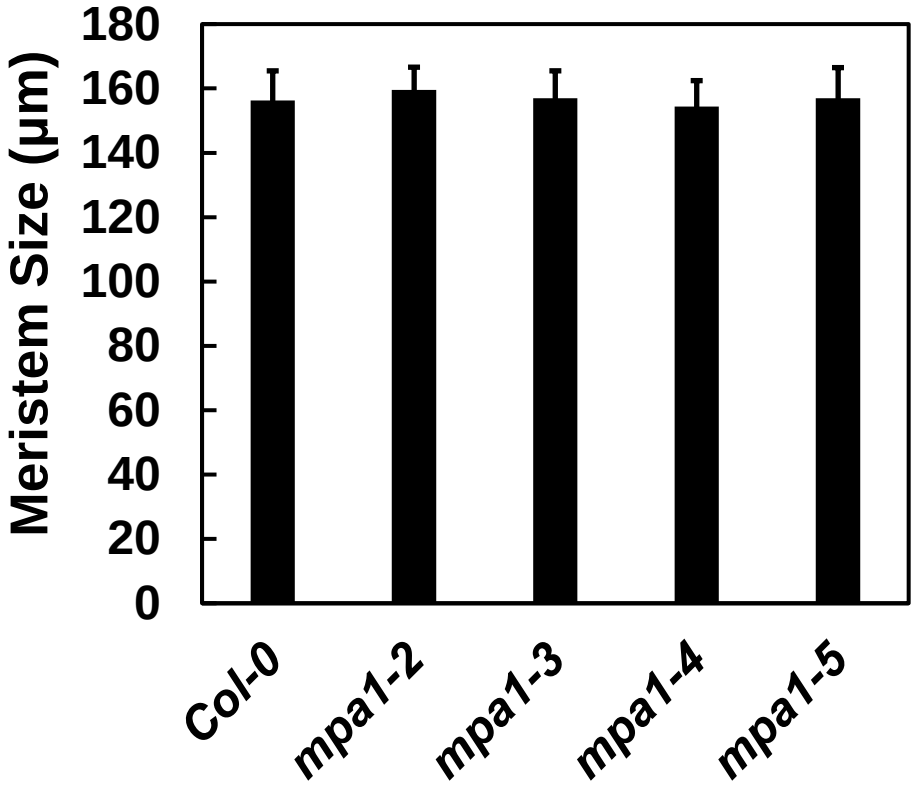

Supplementary Figure 4. Quantification of root meristem size in 5-day old *mpa1*seedlings.

Data are means and standard deviations from three independent experiments (n=10). * P < 0.05 compared to wild type; ANOVA followed Tukey's post-hoc analysis. Variation within groups is higher than variation between groups. The average of meristem size is around 154 to 159 µM for wild type and *mpa1* alleles. The root meristem size of *mpa1* seedlings was not statistically significantly different from Col-0.

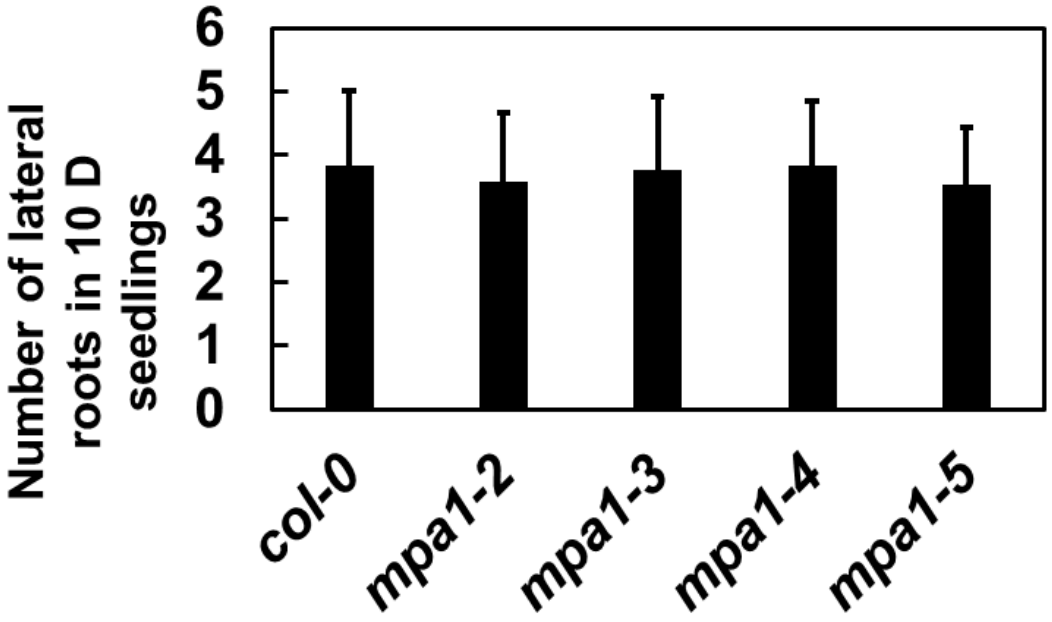

Supplementary Figure 5. Quantification of lateral roots in *mpa1* mutant seedlings.

Data are means and standard deviations from three independent experiments (n=12). * P < 0.05 compared to wild type; ANOVA followed Tukey's post-hoc analysis. Variation within groups was higher than variation between groups. There was no significant difference in lateral root number in *mpa1* compared to Col-0

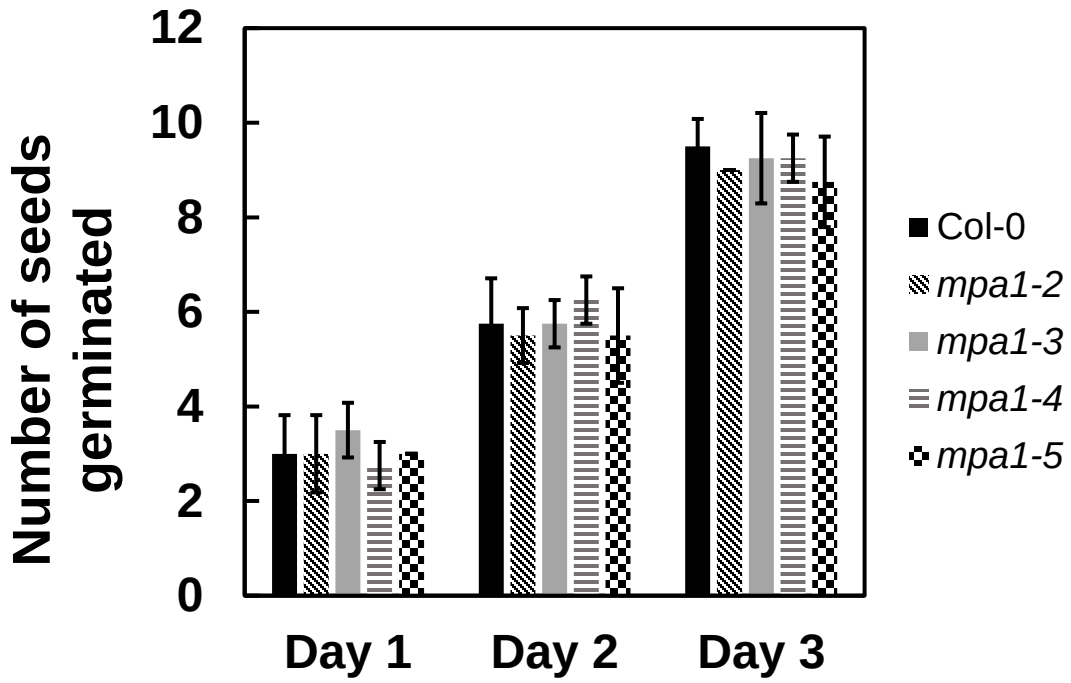

Supplementary Figure 6. Seed germination in *mpa1*.

Data are means and standard deviations from three independent experiments (n=10). * P < 0.05 compared to wild type; ANOVA followed Tukey's post-hoc analysis. Variation within groups is higher than variation between groups. Data indicated that there was no significant difference in number of *mpa1* seeds germinated in each day in comparison to Col-0.

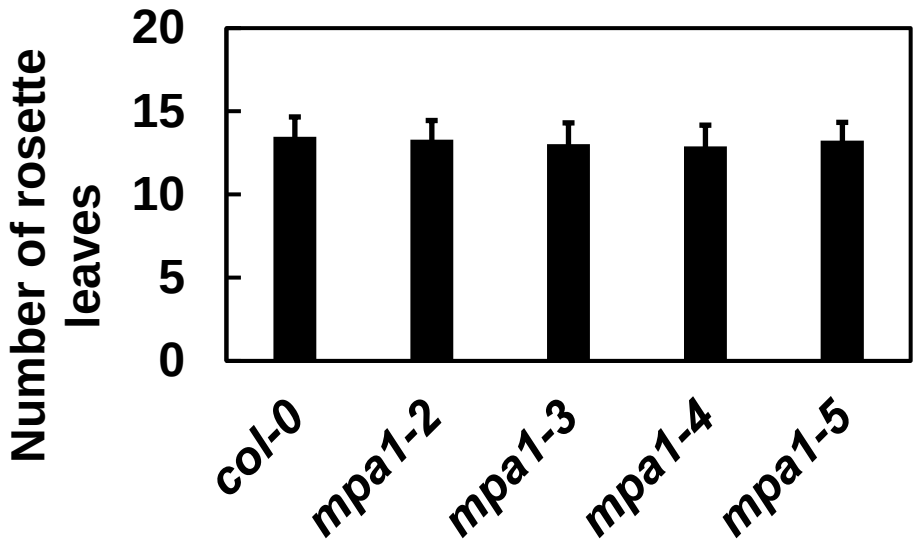

Supplementary Figure 7. Number of rosette leaves in 3 weeks old *mpa1* plants.

Data are means and standard deviations from three independent experiments (n=10). * P < 0.05 compared to wild type; ANOVA followed Tukey's post-hoc analysis. Variation within groups is higher than variation between groups. There was no significant difference in rosette leaf number in *mpa1* compared to Col-0

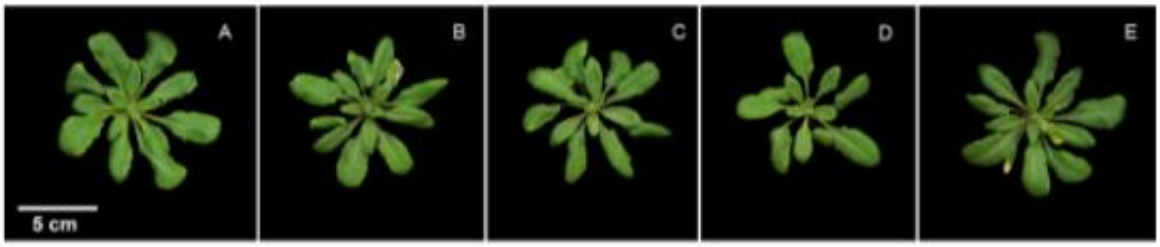

Supplementary Figure 8. Rosette diameter of 3 weeks old *mpa1* individuals.
(A) Col-0 rosette, (B) *mpa1-2* rosette, (C) *mpa1-3* rosette, (D) *mpa1-4* rosette and (E) *mpa1-5* rosette. (Size bar, 5 cm)

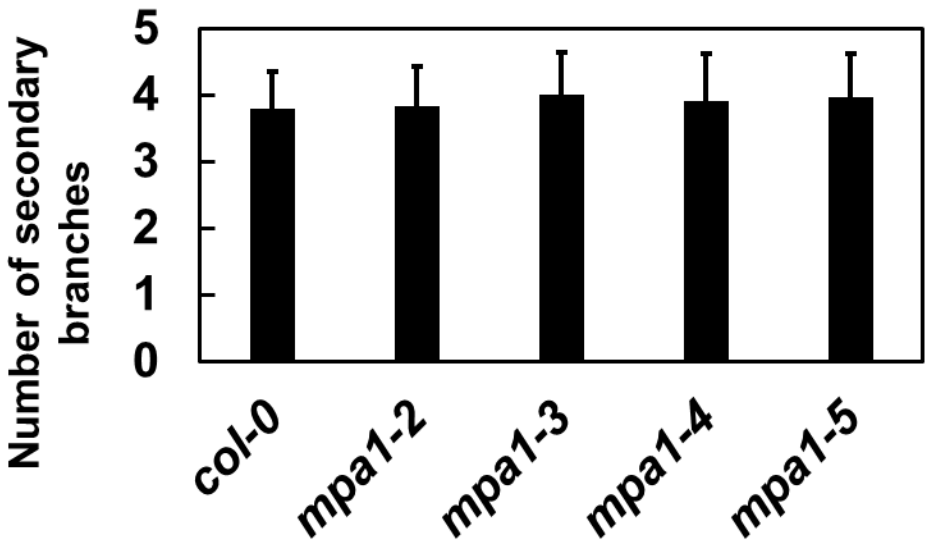

Supplementary Figure 9. Number of secondary branches in 4 weeks old *mpa1* plants. Data are means and standard deviations from 3 independent experiments (n=10). * P < 0.05 compared to wild type; ANOVA followed Tukey's post-hoc analysis. Variation within groups is higher than variation between groups. There was no significant difference in number of secondary branches in mpa1 plants compared to Col-0

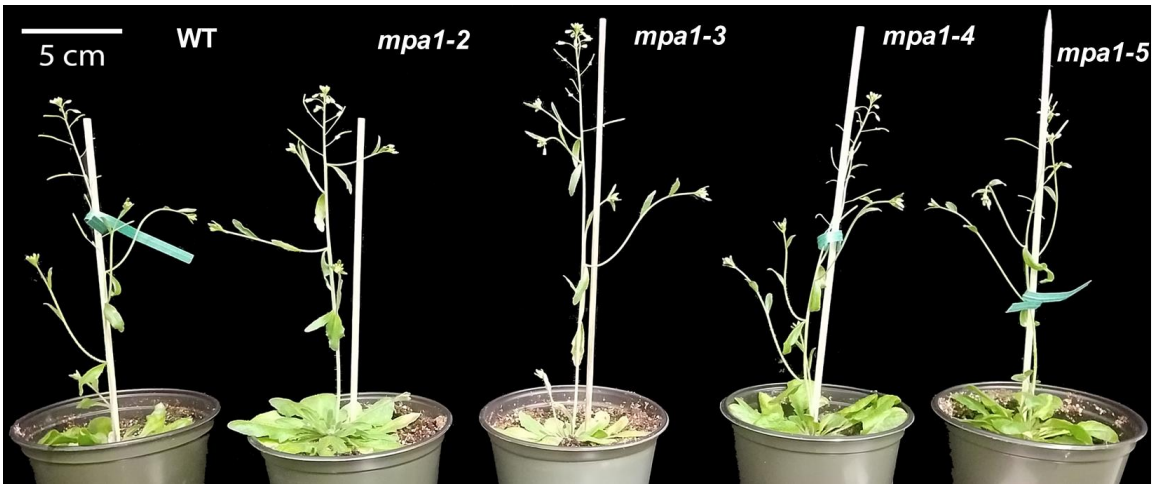

Supplementary Figure 10. Inflorescence height of four week old plants.
(A) Col-0, (B) *mpa1-2*, (C) *mpa1-3* (D) *mpa1-4* (E) *mpa1-5*. Size bar, 5 cm

Bibliography

[1] K. J. Ross, P. Fransz, and G. H. Jones, “A light microscopic atlas of meiosis in *Arabidopsis thaliana*.,” *Chromosome Res.*, vol. 4, no. May, pp. 507–516, 1996.

[2] K. Culligan, A. Tissier, and A. Britt, “ATR Regulates a G2-Phase Cell-Cycle Checkpoint in *Arabidopsis thaliana*,” *Plant Cell*, vol. 16, no. 5, pp. 1091–1104, 2004.

[3] S. A. Osmani, D. B. Engle, J. H. Doonan, and N. R. Morris, “Spindle formation and chromatin condensation in cells blocked at interphase by mutation of a negative cell cycle control gene,” *Cell*, vol. 52, no. 2, pp. 241–251, 1988.

[4] E. Bucciarelli, M. G. Giansanti, S. Bonaccorsi, and M. Gatti, “Spindle assembly and cytokinesis in the absence of chromosomes during *Drosophila* male meiosis,” *J. Cell Biol.*, vol. 160, no. 7, pp. 993–999, 2003.

[5] P. A. Sabelli *et al.*, “Control of cell proliferation, endoreduplication, cell size, and cell death by the retinoblastoma-related pathway in *maize* endosperm,” *Proc. Natl. Acad. Sci.*, vol. 110, no. 19, pp. E1827–E1836, May 2013.

[6] L. Zhao, Y. Li, Q. Xie, and Y. Wu, “Loss of CDKC ; 2 increases both cell division and drought tolerance in *Arabidopsis thaliana*,” *Plant J.*, vol. 91, no. 5, pp. 816–828, Sep. 2017.

[7] V. Boudolf *et al.*, “B1-type cyclin-dependent kinases are essential for the formation of stomatal complexes in *Arabidopsis thaliana*.,” *Plant Cell*, vol. 16, no. 4, pp. 945–55, Apr. 2004.

[8] P. E. Mains, I. A. Sulston, and W. B. Wood, “Dominant maternal-effect mutations causing embryonic lethality in *Caenorhabditis elegans*,” *Genetics*, vol. 125, no. 2, pp. 351–369, 1990.

[9] A. Colon-Carmona, R. You, T. Haimovitch-Gal, and P. Doerner, “Spatio-temporal analysis of mitotic activity with a labile cyclin-GUS fusion protein,” *Plant J.*, vol. 20, no. 4, pp. 503–508, Nov. 1999.

[10] S. U. Andersen *et al.*, “Requirement of B2-type cyclin-dependent kinases for meristem integrity in *Arabidopsis thaliana*.,” *Plant Cell*, vol. 20, no. 1, pp. 88–100, 2008.

[11] K. Vandepoele, J. Raes, L. De Veylder, P. Rouzé, S. Rombauts, and D. Inzé, “Genome-wide analysis of core cell cycle genes in *Arabidopsis*.,” *Plant Cell*, vol. 14, no. 4, pp. 903–16, Apr. 2002.

[12] C. Riou-Khamlichi, M. Menges, J. M. Healy, and J. a Murray, “Sugar control of the plant cell cycle: differential regulation of *Arabidopsis* D-type cyclin gene expression.,” *Mol. Cell. Biol.*, vol. 20, no. 13, pp. 4513–21, Jul. 2000.

[13] W.-H. Shen, “The plant E2F-Rb pathway and epigenetic control.,” *Trends Plant Sci.*, vol. 7, no. 11, pp. 505–11, Nov. 2002.

[14] L. Zhu *et al.*, “Inhibition of cell proliferation by p107, a relative of the retinoblastoma protein.,” *Genes Dev.*, vol. 7, no. 7a, pp. 1111–1125, 1993.

[15] D. G. Johnson, J. K. Schwarz, W. D. Cress, and J. R. Nevins, “Expression of

transcription factor E2F1 induces quiescent cells to enter S phase.," *Nature*, vol. 365, no. 6444, pp. 349–52, 1993.
[16] B. Ren *et al.*, "E2F integrates cell cycle progression with DNA repair, replication, and G(2)/M checkpoints.," *Genes Dev.*, vol. 16, no. 2, pp. 245–56, Jan. 2002.
[17] E. Ramirez-Parra, C. Fründt, and C. Gutierrez, "A genome-wide identification of E2F-regulated genes in *Arabidopsis*," *Plant J.*, vol. 33, no. 4, pp. 801–811, Feb. 2003.
[18] M. Menges, L. Hennig, W. Gruissem, and J. A. H. Murray, "Cell Cycle-regulated Gene Expression in *Arabidopsis*," *J. Biol. Chem.*, vol. 277, no. 44, pp. 41987–42002, Nov. 2002.
[19] M. K. Nowack *et al.*, "Genetic Framework of Cyclin-Dependent Kinase Function in *Arabidopsis*," *Dev. Cell*, vol. 22, no. 5, pp. 1030–1040, May 2012.
[20] B. M. Horvath *et al.*, "*Arabidopsis* RETINOBLASTOMA RELATED directly regulates DNA damage responses through functions beyond cell cycle control," *EMBO J.*, vol. 36, no. 9, pp. 1261–1278, May 2017.
[21] S. Biedermann *et al.*, "The retinoblastoma homolog RBR1 mediates localization of the repair protein RAD51 to DNA lesions in *Arabidopsis*," *EMBO J.*, vol. 36, no. 9, pp. 1279–1297, 2017.
[22] Y. Helariutta *et al.*, "The SHORT-ROOT Gene Controls Radial Patterning of the *Arabidopsis* Root through Radial Signaling," *Cell*, vol. 101, no. 5, pp. 555–567, May 2000.
[23] T. C. Hsu, J. C. Liang, and L. R. Shirley, "Aneuploidy induction by mitotic arrestants," *Mutat. Res. Lett.*, vol. 122, no. 2, pp. 201–209, Nov. 1983.
[24] X. Cai and S. S. Xu, "Meiosis-driven genome variation in plants.," *Curr. Genomics*, vol. 8, no. 3, pp. 151–161, 2007.
[25] B. Huettel, D. P. Kreil, M. Matzke, and A. J. M. Matzke, "Effects of aneuploidy on genome structure, expression, and interphase organization in *Arabidopsis thaliana*," *PLoS Genet.*, vol. 4, no. 10, 2008.
[26] G. Horiguchi, N. Gonzalez, G. T. S. Beemster, D. Inzé, and H. Tsukaya, "Impact of segmental chromosomal duplications on leaf size in the grandifolia-D mutants of *Arabidopsis thaliana*," *Plant J.*, vol. 60, no. 1, pp. 122–133, 2009.
[27] T. L. Burton and B. C. Husband, "Fitness differences among diploids, tetraploids, and their triploid progeny in *Chamerion angustifolium*: mechanisms of inviability and implications for polyploid evolution.," *Evolution*, vol. 54, no. 4, pp. 1182–91, Aug. 2000.
[28] F. Bretagnolle and J. D. Thompson, "An Experimental Study of Ecological Differences in Winter Growth between Sympatric Diploid and Autotetraploid *Dactylis Glomerata*," *J. Ecol.*, vol. 84, no. 3, p. 343, Jun. 1996.
[29] B. C. Husband, "The role of triploid hybrids in the evolutionary dynamics of mixed-ploidy populations," *Biol. J. Linn. Soc.*, vol. 82, no. 4, pp. 537–546, Aug. 2004.
[30] Y. Nagata, Y. Muro, and K. Todokoro, "Thrombopoietin-induced Polyploidization of Bone Marrow Megakaryocytes Is Due to a Unique Regulatory Mechanism in Late Mitosis," *J. Cell Biol.*, vol. 139, no. 2, pp. 449–457, Oct. 1997.
[31] T. Hayashi, T. Sano, N. Kutsuna, F. Kumagai-Sano, and S. Hasezawa,

"Contribution of anaphase B to chromosome separation in higher plant cells estimated by image processing," *Plant Cell Physiol.*, vol. 48, no. 10, pp. 1509–1513, 2007.

[32] I. C. Waizenegger, J. F. Giménez-Abián, D. Wernic, and J.-M. Peters, "Regulation of Human Separase by Securin Binding and Autocleavage," *Curr. Biol.*, vol. 12, no. 16, pp. 1368–1378, Aug. 2002.

[33] S. Wu, W.-R. Scheible, D. Schindelasch, H. Van Den Daele, L. De Veylder, and T. I. Baskin, "A conditional mutation in *Arabidopsis thaliana* separase induces chromosome non-disjunction, aberrant morphogenesis and cyclin B1;1 stability," *Development*, vol. 137, no. 6, pp. 953–961, 2010.

[34] F. Bretagnolle and R. Lumaret, "Bilateral polyploidization in *Dactylis glomerata* L. subsp. lusitanica: occurrence, morphological and genetic characteristics of first polyploids," *Euphytica*, vol. 84, no. 3, pp. 197–207, 1995.

[35] N. P. Trust and T. N. Phytologist, "Diploid-Tetraploid Sympatry in *Dactylis* (Gramineae) Author (s): Martin Borrill and Ruth Lindner Source : The New Phytologist , Vol . 70 , No . 6 (Nov ., 1971), pp . 1111-1124 Published by : Wiley on behalf of the New Phytologist Trust Stable URL : h," vol. 70, no. 6, pp. 1111–1124, 2017.

[36] X. Gu, "Evolution of duplicate genes versus genetic robustness against null mutations," *Trends Genet.*, vol. 19, no. 7, pp. 354–356, 2003.

[37] R. Hovav *et al.*, "The evolution of spinnable cotton fiber entailed prolonged development and a novel metabolism," *PLoS Genet.*, vol. 4, no. 2, 2008.

[38] D. L. Auger, A. D. Gray, T. S. Ream, A. Kato, E. H. Coe, and J. A. Birchler, "Nonadditive gene expression in diploid and triploid hybrids of maize," *Genetics*, vol. 169, no. 1, pp. 389–397, 2005.

[39] B. K. Mable and S. P. Otto, "Masking and purging mutations following EMS treatment in haploid, diploid and tetraploid yeast (*Saccharomyces cerevisiae*)," *Genet. Res.*, vol. 77, no. 1, p. S0016672300004821, 2001.

[40] T. Cavalier-Smith, "Nuclear volume control by nucleoskeletal DNA, selection for cell volume and cell growth rate, and the solution of the DNA C-value paradox," *J. Cell Sci.*, vol. 34, pp. 247–278, 1978.

[41] I. Mastenbroek, J. M. Dewet, and C. Y. Lu, "Chromosome behaviour in early and advanced generations of tetraploid *maize*," *Caryologia*, vol. 35, no. 4, pp. 463–470, 1982.

[42] N. Agrawal and M. a Brown, "Genetic associations and functional characterization of M1 aminopeptidases and immune-mediated diseases," *Genes Immun.*, vol. 15, no. 8, pp. 521–527, Dec. 2014.

[43] A. Catalano, Y. Poloz, and D. H. O'Day, "*Dictyostelium* puromycin-sensitive aminopeptidase A is a nucleoplasmic nucleomorphin-binding protein that relocates to the cytoplasm during mitosis," *Histochem. Cell Biol.*, vol. 136, no. 6, pp. 677–688, 2011.

[44] M. Q. Granato, P. de Araújo Massapust, S. Rozental, C. S. Alviano, A. L. S. dos Santos, and L. F. Kneipp, "1,10-Phenanthroline Inhibits the Metallopeptidase Secreted by *Phialophora verrucosa* and Modulates its Growth, Morphology and Differentiation," *Mycopathologia*, vol. 179, no. 3–4, pp. 231–242, 2015.

[45] J. González-Bacerio *et al.*, "High-level expression in Escherichia coli, purification and kinetic characterization of *Plasmodium falciparum* M1-aminopeptidase," *Protein Expr. Purif.*, vol. 104, pp. 103–114, Dec. 2014.
[46] S. Gras *et al.*, "Aminopeptidase N1 (EtAPN1), an M1 metalloprotease of the apicomplexan parasite *Eimeria tenella*, participates in parasite development," *Eukaryot. Cell*, vol. 13, no. 7, pp. 884–895, 2014.
[47] K. B. Maynard, S. A. Smith, A. C. Davis, A. Trivette, and R. L. Seipelt-Thiemann, "Evolutionary analysis of the mammalian M1 aminopeptidases reveals conserved exon structure and gene death," *Gene*, vol. 552, no. 1, pp. 126–132, 2014.
[48] E. Sánchez-Morán, G. H. Jones, F. C. H. Franklin, and J. L. Santos, "A puromycin-sensitive aminopeptidase is essential for meiosis in Arabidopsis thaliana.," *Plant Cell*, vol. 16, no. 11, pp. 2895–2909, 2004.
[49] F. N. Hosein, A. Bandyopadhyay, W. A. Peer, and A. S. Murphy, "The Catalytic and Protein-Protein Interaction Domains Are Required for APM1 Function," *Plant Physiol.*, vol. 152, no. 4, pp. 2158–2172, 2010.
[50] W. A. Peer *et al.*, "Mutation of the membrane-associated M1 protease APM1 results in distinct embryonic and seedling developmental defects in *Arabidopsis*.," *Plant Cell*, vol. 21, no. 6, pp. 1693–1721, 2009.
[51] W. Kramer *et al.*, "Aminopeptidase N (CD13) is a molecular target of the cholesterol absorption inhibitor ezetimibe in the enterocyte brush border membrane.," *J. Biol. Chem.*, vol. 280, no. 2, pp. 1306–20, Jan. 2005.
[52] D. E. Wentworth and K. V Holmes, "Molecular determinants of species specificity in the coronavirus receptor aminopeptidase N (CD13): influence of N-linked glycosylation.," *J. Virol.*, vol. 75, no. 20, pp. 9741–52, Oct. 2001.
[53] M. Pradillo, E. López, C. Romero, E. Sánchez-Morán, N. Cuñado, and J. L. Santos, "An analysis of univalent segregation in meiotic mutants of *Arabidopsis* thaliana: A possible role for synaptonemal complex," *Genetics*, vol. 175, no. 2, pp. 505–511, 2007.
[54] C. Ma *et al.*, "Novel leucine ureido derivatives as aminopeptidase N inhibitors. Design, synthesis and activity evaluation," *Eur. J. Med. Chem.*, vol. 108, pp. 21–27, 2016.
[55] M. Löhn, C. Mueller, and J. Langner, "Cell Cycle Retardation in Monocytoid Cells Induced by Aminopeptidase N (CD13)," *Leuk. Lymphoma*, vol. 43, no. 2, pp. 407–413, Jan. 2002.
[56] J. Tang *et al.*, "Molecular characterization and dietary regulation of aminopeptidase N (APN) in the grass carp (*Ctenopharyngodon idella*)," *Gene*, vol. 582, no. 1, pp. 77–84, May 2016.
[57] C. Santiago *et al.*, "Allosteric inhibition of aminopeptidase N functions related to tumor growth and virus infection," *Nat. Publ. Gr.*, pp. 1–14, 2017.
[58] L. Bodineau *et al.*, "Orally active aminopeptidase A inhibitors reduce blood pressure: A new strategy for treating hypertension," *Hypertension*, vol. 51, no. 5, pp. 1318–1325, 2008.
[59] M. J. Althoff, K. Flick, and C. Trzepacz, "Collaboration within the M1 aminopeptidase family promotes reproductive success in *Caenorhabditis elegans*," *Dev. Genes Evol.*, vol. 224, no. 3, pp. 137–146, May 2014.

[60] S. M. Fortin *et al.*, “The PAM-1 aminopeptidase regulates centrosome positioning to ensure anterior–posterior axis specification in one-cell *C. elegans* embryos,” *Dev. Biol.*, vol. 344, no. 2, pp. 992–1000, Aug. 2010.
[61] S. Wu, B. Liu, Z. Yuan, X. Zhang, and H. Liu, “Planarian homolog of puromycin-sensitive aminopeptidase *DjPsa* is required for brain regeneration,” *Invertebr. Neurosci.*, vol. 17, no. 2, pp. 1–8, 2017.
[62] D. R. Brooks, N. M. Hooper, and R. E. Isaac, “The *Caenorhabditis* elegans Orthologue of Mammalian Puromycin-sensitive Aminopeptidase Has Roles in Embryogenesis and Reproduction,” *J. Biol. Chem.*, vol. 278, no. 44, pp. 42795–42801, Oct. 2003.
[63] A. S. Murphy, K. R. Hoogner, W. A. Peer, and L. Taiz, “Identification, purification, and molecular cloning of N-1-naphthylphthalmic acid-binding plasma membrane-associated aminopeptidases from *Arabidopsis*.,” *Plant Physiol.*, vol. 128, no. 3, pp. 935–50, Mar. 2002.
[64] F. A. Kaffarnik, A. M. Jones, J. P. Rathjen, and S. C. Peck, “Effector proteins of the bacterial pathogen *Pseudomonas syringae* alter the extracellular proteome of the host plant, Arabidopsis thaliana,” *Mol Cell Proteomics*, vol. 8, no. 1, pp. 145–156, 2009.
[65] B. Cooper, K. B. Campbell, J. Feng, W. M. Garrett, and R. Frederick, “Nuclear proteomic changes linked to soybean rust resistance.,” *Mol. Biosyst.*, vol. 7, no. 3, pp. 773–83, Mar. 2011.
[66] E. Truernit *et al.*, “High-Resolution Whole-Mount Imaging of Three-Dimensional Tissue Organization and Gene Expression Enables the Study of Phloem Development and Structure in *Arabidopsis*,” *Plant Cell Online*, vol. 20, no. 6, pp. 1494–1503, 2008.
[67] M. G. Murray and W. F. Thompson, “Rapid isolation of high molecular weight plant DNA,” *Nucleic Acids Res.*, vol. 8, no. 19, pp. 4321–4326, 1980.
[68] C. Grefen, N. Donald, K. Hashimoto, J. Kudla, K. Schumacher, and M. R. Blatt, “A ubiquitin-10 promoter-based vector set for fluorescent protein tagging facilitates temporal stability and native protein distribution in transient and stable expression studies,” *Plant J.*, vol. 64, no. 2, pp. 355–365, 2010.
[69] S. J. Clough and A. F. Bent, “Floral dip: A simplified method for *Agrobacterium*-mediated transformation of *Arabidopsis thaliana*,” *Plant J.*, vol. 16, no. 6, pp. 735–743, 1998.
[70] N. De Storme, B. N. Keçeli, L. Zamariola, G. Angenon, and D. Geelen, “CENH3-GFP: a visual marker for gametophytic and somatic ploidy determination in *Arabidopsis thaliana*.,” *BMC Plant Biol.*, vol. 16, no. 1, p. 1, 2016.
[71] J. Doležel, J. Greilhuber, and J. Suda, “Estimation of nuclear DNA content in plants using flow cytometry,” *Nat. Protoc.*, vol. 2, no. 9, pp. 2233–2244, 2007.
[72] J. G. Walling, R. Shoemaker, N. Young, J. Mudge, and S. Jackson, “Chromosome-level homeology in paleopolyploid soybean (*Glycine max)* revealed through integration of genetic and chromosome maps,” *Genetics*, vol. 172, no. 3, pp. 1893–1900, 2006.
[73] W. H. Pan, A. Houben, and R. Schlegel, “Highly effective cell synchronization in plant roots by hydroxyurea and amiprophos-methyl or colchicine,” *Genome*, vol.

36, no. 2, pp. 387–390, 1993.
[74] C. Lincoln, “A knotted1-like Homeobox Gene in Arabidopsis Is Expressed in the Vegetative Meristem and Dramatically Alters Leaf Morphology When Overexpressed in Transgenic Plants,” *Plant Cell Online*, vol. 6, no. 12, pp. 1859–1876, 1994.
[75] E. S. Coen, J. Romero, S. Doyle, R. Elliott, G. Murphy, and R. Carpenter, “floricaula: A homeotic gene required for flower development in antirrhinum majus,” *Cell*, vol. 63, no. 6, pp. 1311–1322, 1990.
[76] D. W. Galbraith, “Endoreduplicative standards for calibration of flow cytometric C-Value measurements,” *Cytom. Part A*, vol. 85, no. 4, pp. 368–374, 2014.
[77] E. Allen, Z. Xie, A. M. Gustafson, and J. C. Carrington, “microRNA-directed phasing during trans-acting siRNA biogenesis in plants,” *Cell*, vol. 121, no. 2, pp. 207–221, 2005.
[78] P. M. Waterhouse, M. W. Graham, and M.-B. Wang, “Virus resistance and gene silencing in plants can be induced by simultaneous expression of sense and antisense RNA,” *Proc. Natl. Acad. Sci. U. S. A.*, vol. 95, no. 23, pp. 13959–13964, 1998.
[79] A. Madlung, “Polyploidy and its effect on evolutionary success: old questions revisited with new tools,” *Heredity (Edinb).*, vol. 110, no. 2, pp. 99–104, Feb. 2013.
[80] J. A. Birchler, “Aneuploidy in plants and flies: The origin of studies of genomic imbalance,” *Semin. Cell Dev. Biol.*, vol. 24, no. 4, pp. 315–319, 2013.
[81] J. E. Melaragno, “Relationship between Endopolyploidy and Cell Size in Epidermal Tissue of *Arabidopsis*,” *Plant Cell Online*, vol. 5, no. 11, pp. 1661–1668, 1993.
[82] G. Linc, E. Gaal, I. Molnar, D. Icsoa, E. Badaeva, and M. Molnaar-Lang, “Molecular cytogenetic (FISH) and genome analysis of diploid wheatgrasses and their phylogenetic relationship,” *PLoS One*, vol. 12, no. 3, pp. 1–18, 2017.
[83] L. Comai, “Phenotypic Instability and Rapid Gene Silencing in Newly Formed Arabidopsis Allotetraploids,” *Plant Cell Online*, vol. 12, no. 9, pp. 1551–1568, 2000.
[84] I. M. Henry, B. P. Dilkes, K. Young, B. Watson, H. Wu, and L. Comai, “Aneuploidy and genetic variation in the *Arabidopsis thaliana* triploid response,” *Genetics*, vol. 170, no. 4, pp. 1979–1988, 2005.
[85] H. Levanony, R. Rubin, Y. Altschuler, and G. Galili, “Evidence for a novel route of wheat storage proteins to vacuoles,” *J. Cell Biol.*, vol. 119, no. 5, pp. 1117–1128, 1992.